New insights into widely linear MMSE receivers for communication networks using data-like rectilinear or quasi-rectilinear signals

Pascal Chevalier, Jean-Pierre Delmas, Roger Lamberti

New insights into widely linear MMSE receivers for communication networks using data-like rectilinear or quasi-rectilinear signals

Pascal Chevalier, Jean-Pierre Delmas, and Roger Lamberti

***Abstract*—Widely linear (WL) processing has been of great interest these last two decades for multi-user (MUI) interference mitigation in radiocommunications networks using rectilinear (R) or quasi-rectilinear (QR) signals in particular. Despite numerous papers on the subject, this topic remains of interest for several current and future applications which use R or QR signals, described hereafter. In this context, using a continuous time approach, it is shown in this paper the sub-optimality of most of the WL MMSE receivers of the literature, which are implemented at the symbol rate after a matched filtering operation to the pulse shaping filter, and the necessity to know the MUI channels, always cumbersome in practice, to implement the optimal WL MMSE receiver. Then, the main challenge addressed in the paper is to propose new WL MMSE receivers able to implement the optimal one without requiring the MUI channels knowledge. For this purpose, two new WL MMSE receivers, a two-input one and a three-input one, are proposed and analyzed in this paper for R and QR signals corrupted by data-like MUI. The two-input and three-input receivers are shown to be quasi-optimal respectively for R signals using Square Root Raised Cosine (SRRC) filters with a low roll-off and for R and QR signals whatever the pulse shaping filter, showing in particular the non-equivalence of R and QR signals for WL MMSE receivers. These two new receivers open new perspectives for the implementation of the optimal WL MMSE receiver in the presence of data-like MUI from the only knowledge of the SOI channel.**

***Index Terms*—Non circular, Widely linear, MMSE, Rectilinear, Quasi-Rectilinear, SAIC/MAIC, MUI, ISI, Continous-Time, two-input, three-input, FRESH, MSK, GMSK, OQAM, ASK, BPSK**

Paper accepted in IEEE Trans. Signal Processing
October 8, 2024

I. Introduction

WIDELY linear (WL) processing [1] has been of great interest these last two decades for many applications involving second-order (SO) non-circular (or improper) signals [2] and for data-like multi-user interference (MUI) and multi-antenna interference (MAI) mitigation in radiocommunication networks using rectilinear (R) or quasi-rectilinear (QR) signals in particular. Let us recall that R signals correspond to mono-dimensional signals, or real-valued signals to a potential phase term, such as amplitude modulated (AM), amplitude shift keying (ASK) or binary phase shift keying (BPSK) signals, whereas QR signals are complex signals corresponding, after a simple derotation operation [3], to a complex filtering of an R signal. Examples of QR signals are signals using π/2-BPSK, minimum shift keying (MSK) or offset quadrature amplitude (OQAM) modulations, while an example of approximated QR signal is a signal using the Gaussian MSK (GMSK) modulation. For data-like R or QR MUI or MAI, a well-suited WL receiver implemented from N antennas creates N additional virtual antennas and generates a virtual array of $2N$ antennas, allowing to discriminate the received sources by the phase, in addition to the spatial discrimination available for $N > 1$ [4]. It then allows the potential rejection of $2N-1$ (instead of $N-1$ for linear receivers) data-like MUI or MAI, and a Single Antenna Interference Cancellation (SAIC) capability from a single antenna reception [4], hence its great practical interest.

For this reason, WL processing has been considered in the past for R MUI and narrow-band interference (NBI) mitigation in code division multiple access (CDMA) networks [5], [6], in orthogonal frequency division multiplex systems [7] and in ultra wide band networks [8] in particular. It has also been proposed for R MAI suppression in V-BLAST single user Muti-Input Multi-Output (MIMO) systems [9], [10] and for R MUI mitigation in MIMO systems using spatio-temporal block coding [11]. Moreover, since the end of the nineties, WL processing has also been proposed for QR MUI mitigation in CDMA networks using offset quadrature phase shift keying (OQPSK) modulation [12]. It has also been strongly studied and applied for single/multiple antenna interference cancellation (SAIC/MAIC) in radiocommunication networks using QR signals, and in the GSM cellular networks in particular, which use the GMSK modulation. Several SAIC WL receivers, allowing the separation of two users from only one receive antenna, have been

P. Chevalier is with CNAM, laboratoire CEDRIC, HESAM University, 292 rue Saint Martin, 75141 Paris Cedex 3, France and also with Thales France, HTE/AMS/TCP, 4 Av. Louvresses, 92622 Gennevilliers, Cedex, France e-mail: pascal.chevalier@cnam.fr, pascal.chevalier@thalesgroup.com.

J.-P. Delmas is with Samovar laboratory, Telecom SudParis, Institut Polytechnique de Paris, 91120 Palaiseau, France, e-mail: jean-pierre.delmas@it-sudparis.eu.

R. Lamberti is with CITI department, Telecom SudParis, Institut Polytechnique de Paris, 91120 Palaiseau, France, e-mail: roger.lamberti@orange.fr.

proposed in [4], [13], [14] and inserted in most of GSM handsets since 2006 [15], allowing significant capacity gains in GSM networks [14], [16]. Other WL receivers have also been proposed for SAIC [17], [18] and SAIC/MAIC [19] in voice services over adaptive multi-user channels on one slot (VAMOS) networks, a standardized extension of GSM networks, aiming at increasing the capacity of GSM, while maintaining backward compatibility with the legacy system.

Despite these numerous papers about WL processing for R and QR MUI or MAI mitigation, this topic remains of great interest for several current and future applications. This concerns in particular anti-collisions processing in radio frequency identification systems [20] or in dense machine-type networks such as grant-free narrow-band internet of things (IoT) networks for uplink transmissions [21], which use R and QR signals respectively, and in satellite-AIS systems for maritime surveillance which use GMSK signals [22]. This topic is also relevant to allow 5G and beyond 5G (B5G) networks to support a massive number of low data rate devices through one-dimensional signaling [23], potentially jointly with MIMO non-orthogonal multiple access (MIMO-NOMA) systems [24], or fully or over-loaded large MU-MIMO systems using R signals [25]. Moreover, QR interference mitigation by WL processing remains also of great interest for unmanned aerial vehicles (UAVs or drones), who are expected to become one of the important enabling technologies for B5G cellular networks and whose applications development is growing dramatically for many civilian applications (monitoring, surveillance, traffic control, relaying etc..) [26]. Indeed, the bidirectional Control and Non Payload Communications (CNPC) link, connecting the ground control station to the UAV, which is a safety-critical link requiring improved receivers in terms of reliability, availability and low latency in a large variety of environmental and propagation conditions, uses the GMSK modulation [27]. In low-altitude operations, CNPC links meet frequency selective wireless channels and WL processing is of interest for channel equalization, as already described in [27]. In order to reduce the size, and then the complexity, of the equalizer, an additional interest of WL processing may be to potentially cancel the multiple paths arriving outside the equalizer length, thus considered as MUI. Another application where QR interference mitigation by WL processing may be still of interest concerns communication networks using FBMC-OQAM waveforms [28] candidate for beyond 5G and future Internet of Things networks [29], thanks to their good frequency localization and compatibility with asynchronous links. For frequency selective channel, FBMC-OQAM waveforms generate Inter-Carrier Interference (ICI) at reception, which may be processed by efficient WL processing. Preliminary WL based solutions for FBMC-OQAM waveforms are presented in [30], [31] for MIMO links using spatial multiplexing at transmission and in [32] for SISO links.

In this challenging context, let us note that most of the WL receivers currently available in the literature for R or QR MUI, MAI or ICI mitigation are WL MMSE receivers. Although these receivers have been strongly studied these two last decades, several important questions related to the relevance of their structure, their performance, their implementation requirements and their potential equivalence for R and QR signals remain surprisingly raised. More precisely, except for those presented in [12] and [19], most of the other WL MMSE receivers are implemented at the symbol rate, after a matched filtering operation to the pulse shaping filter and have thus a particular structure constraint (sc). Among these constrained receivers, [9], [10], [20], [21], [23], [25], [30] fully exploit the similar waveform of SOI and MUI by jointly estimating the SOI and interference symbols, which requires the a priori knowledge or estimation of both the SOI and MUI channels. Other WL MMSE receivers [4]–[8], [14], [17], [18], [31], [32] estimate the SOI symbols only, which does not require the a priori knowledge or estimation of the MUI channels. In this context, the first contribution of this paper is to show, for both R and QR signals and under the previous structure constraint, the equivalence of these two approaches for both the linear (L) (or one-input) and the WL (or two-input) MMSE receivers, thus discarding the need to know or to estimate in this case the MUI channel responses, always cumbersome in practice. The previous receivers are called in the following sc M-input receivers with $M = 1$ and 2 respectively. As only R and QR signals are considered, only WL receivers are of interest in this paper, whereas L receivers are only considered as reference receivers. The second contribution of this paper is to compute, for R and QR signals and for $M = 1, 2$, the M-input MMSE receiver without any structure constraint, called optimal M-input MMSE receiver and denoted by o M-input MMSE receiver. The o M-input receiver is very scarcely considered in the literature. It fully exploits the MUI waveform knowledge and implicitly exploits all the cyclostationarity properties of the MUI, in addition to their SO non-circularity for $M = 2$. However, contrary to the sc M-input MMSE receiver, the o M-input MMSE receiver requires the a priori knowledge or estimation of the MUI channels, which is one of its main limitations. The third contribution of this paper is to show, for R and QR signals and for $M = 1, 2$, the general sub-optimality of the sc M-input MMSE receiver, yet mainly used in the literature, which thus cannot implement the o M-input MMSE receiver in most cases. It then becomes interesting to propose new M-input MMSE receivers able to implement the o M-input MMSE receiver but without requiring the knowledge of the MUI channels. In this context, the main contributions of this paper is to propose, for both R and QR signals, two new WL MMSE receivers aiming at implementing the o two-input MMSE receiver but without requiring the MUI channels. The first receiver, which constitutes the fourth

contribution of this paper, is a two-input MMSE receiver, called s two-input MMSE receiver, having no structure constraint but assuming a false stationarity property of the MUI. This receiver does not require the knowledge of the MUI channels, hence its practical interest. However, the performance analysis of this receiver, presented in this paper, shows its quasi-optimality for R signals using SRRC filters with weak roll-off but its increasing sub-optimality as the roll-off increases. Moreover, this receiver is shown to be always sub-optimal for QR signals, showing in particular the non-equivalence of R and QR signals for WL MMSE processing, contrary to what is implicitly assumed in most of papers dealing with WL processing of QR signals. For this reason, a second receiver, which constitutes the fifth contribution of this paper, and corresponding to a three-input WL frequency shifted (FRESH) receiver, is proposed in this paper. This receiver, called s three-input MMSE receiver, is shown to be quasi-optimal for both R and QR signals, for most filters and propagation channels, allowing to quasi-implement the o two-input MMSE receiver without the need to know the MUI channels, which seems to be unprecedented and which opens new perspectives for the implementation of the latter.

To introduce the previous receivers we adopt a continuous-time (CT) approach which is justified by three reasons. The first one, is that implementation issues are out of the scope of the paper, which is mainly conceptual but which may be a prerequisite for implementation optimizations investigated elsewhere. The second one, is that a CT approach allows us to remove the potential influence of the sample rate imposed by a discrete-time (DT) approach. The third one, is that it allows us to obtain analytical and potentially interpretable expressions for the output performance of the receivers considered in the paper, which are completely original and which constitute the sixth contribution of this paper. Note that a three-input WL FRESH receiver has already been proposed in [33] and [34] for QR data-like MUI mitigation, both without and with frequency offset respectively, but using a pseudo Maximum Likelihood Sequence Estimation (MLSE) approach. This gives rise to the three-input WL pseudo-MLSE receiver much more heavy to implement than the three-input WL MMSE receiver introduced in this paper. Moreover, note that the MMSE-based M-input FRESH receiver introduced in [35] for co-channel interference (CCI) mitigation, also called M-input cyclic Wiener receiver, is very different from the receivers introduced in this paper. Indeed the M-input cyclic Wiener receiver of [35] is the solution of an MMSE estimation problem and generates the best M-input MMSE estimate of a CT digital signal in the presence of cyclostationary CCI. On the contrary, the different MMSE receivers considered in this paper are equalizers rather than signal estimators and generate M-input $(M = 1, 2, 3)$ MMSE estimates of the received useful symbols under different assumptions on the MUI and receiver structure. None of the receivers introduced in this paper is considered in [35] which, in addition, does not mention QR signals and does not present any analytical performance results.

The paper is organized as follows. Section II introduces the observation model and the extended one for both two-input and three-input WL processing of both R and QR signals, jointly with the SO statistics of the total noise. Section III derives, for R and QR signals, the sc and o M-input $(M = 1, 2)$ and the s M-input $(M = 1, 2, 3)$ MMSE receivers. Section IV gives, for R and QR signals, general closed-form expressions of the SINR on the current symbol at the real-part output of these derived receivers. Section **??** considers the presence of zero and one data-like MUI and gives very insightful analytical interpretable expressions of these SINRs in some particular cases, which is very original. A comparative analysis of these SINR is then presented, both analytically and by computer simulations, for several propagation channels, and several kinds of signals, which is the seventh contribution of this paper. Section V shows that the results obtained through the output SINR criterion are still valid for the output symbol error rate (SER). Finally Section VI concludes this paper.

Notations: Before proceeding, we fix the notations used throughout the paper. Non boldface symbols are scalar whereas lower (upper) case boldface symbols denote column vectors (matrices). T, H and $*$ means the transpose, conjugate transpose and conjugate, respectively. $\otimes$ is the convolution operation. $\delta(x)$ is the Kronecker symbol such that $\delta(x) = 1$ for $x = 0$ and $\delta(x) = 0$ for $x \neq 0$. $\mathbf{0}_K$ and $\mathbf{I}_K$ are the zero and the identity matrices of dimension K, respectively. Moreover, all Fourier transforms of vectors $\mathbf{x}$ and matrices $\mathbf{X}$ use the same notation where time parameters t or τ is simply replaced by frequency f.

II. Models and total noise second-order statistics

A. Observation model and total noise SO statistics

A1) *Observation model:* We consider an array of N narrow-band antennas receiving the contribution of a SOI, which may be R or QR, P data-like MUI, having the same nature (R or QR), the same symbol period and the same pulse-shaping filter as the SOI, and a background noise. The $N \times 1$ vector of complex amplitudes of the data at the output of these antennas after frequency synchronization can then be written as

$$\begin{aligned}\mathbf{x}(t) &= \sum_{\ell} a_\ell \mathbf{g}(t-\ell T) + \sum_{1\leq p\leq P} \sum_{\ell} a_{p,\ell} \mathbf{g}_p(t-\ell T) + \boldsymbol{\epsilon}(t) \\ &= \sum_{\ell} \mathbf{G}(t-\ell T)\mathbf{a}_\ell + \boldsymbol{\epsilon}(t) \stackrel{\text{def}}{=} \sum_{\ell} a_\ell \mathbf{g}(t-\ell T) + \mathbf{n}(t) \quad (1)\end{aligned}$$

Here, $(a_\ell, a_{p,\ell}) = (b_\ell, b_{p,\ell})$ for R signals, whereas $(a_\ell, a_{p,\ell}) = (j^\ell b_\ell, j^\ell b_{p,\ell})$ for QR signals, where b_ℓ and

$b_{p,\ell}$ $(1 \leq p \leq P)$ are real-valued zero-mean independent identically distributed (i.i.d.) random variables, corresponding to the SOI and MUI p symbols respectively for R signals and directly related to the SOI and MUI p symbols, respectively for QR signals [36]–[38], T is the symbol period for R, $\pi/2$-BPSK, $\pi/2$-ASK, MSK and GMSK signals [37], [38] and half the symbol period for OQAM signals [36], $\mathbf{g}(t) = v(t) \otimes \mathbf{h}(t)$ is the $N \times 1$ impulse response vector of the SOI global channel, $v(t)$ and $\mathbf{h}(t)$ are respectively the scalar and $N \times 1$ impulse responses of the SOI pulse shaping filter and propagation channel, respectively, $\mathbf{g}_p(t) \stackrel{\text{def}}{=} v(t) \otimes \mathbf{h}_p(t)$ where $\mathbf{h}_p(t)$ is the impulse response vector of the propagation channel of the MUI p, $\mathbf{G}(t)$ is the $N \times (P+1)$ matrix defined by $\mathbf{G}(t) \stackrel{\text{def}}{=} [\mathbf{g}(t), \mathbf{g}_1(t), ..., \mathbf{g}_p(t)] = v(t) \otimes \mathbf{H}(t)$ where $\mathbf{H}(t) \stackrel{\text{def}}{=} [\mathbf{h}(t), \mathbf{h}_1(t), ..., \mathbf{h}_p(t)]$, $\mathbf{a}_\ell$ is the $(P+1) \times 1$ vector defined by $\mathbf{a}_\ell \stackrel{\text{def}}{=} [a_\ell, a_{1,\ell}, ..., a_{P,\ell}]^T$, $\boldsymbol{\epsilon}(t)$ is the $N \times 1$ background noise vector assumed to be zero-mean, circular, stationary, temporally and spatially white and $\mathbf{n}(t)$ is the total noise vector composed of the P MUI and background noise. Note that model (1) with $(a_\ell, a_{p,\ell}) = (j^\ell b_\ell, j^\ell b_{p,\ell})$ is exact for $\pi/2$-BPSK, $\pi/2$-ASK, MSK and OQAM signals whereas it is only an approximated model for GMSK signals [37].

For R signals, the filter $v(t)$ is assumed to correspond to a normalized (with unit-energy) square root raised cosine (SRRC) filter with a roll-off ω and a bandwidth $B = (1+\omega)/T$. For QR signals, four normalized filters $v(t)$ are considered, depending on the QR constellation. For $\pi/2$-BPSK or $\pi/2$-ASK constellations, $v(t)$ is the same as for R signals. For OQAM signals, $v(t)$ is also a normalized SRRC filter but for the symbol duration $2T$ instead of T. For a MSK signal, $v(t)$ is defined by

$$v(t) = \begin{cases} \frac{1}{\sqrt{T}} \sin(\frac{\pi t}{2T}), & t \in [0, 2T] \\ 0, & \text{elsewhere,} \end{cases} \quad (2)$$

whereas for a GMSK signal, $v(t)$ is, ideally, approximately defined by the $c_0(t)$ pulse of the Laurent decomposition [37]. However, as $c_0(t)$ is a complicate function of t, in this paper we approximate this pulse by the following Gaussian filter

$$v(t) \approx \frac{1}{(\sigma T \sqrt{2\pi})^{1/2}} \; e^{-\frac{(t-2T)^2}{4(\sigma T)^2}}, \quad (3)$$

where σ has to be chosen to approximate $c_0(t)$. The value $\sigma = 1$ seems to be a good choice [13].

A2) *Total Noise SO statistics:* The SO statistics of $\mathbf{n}(t)$ are characterized by the two correlation matrices $\mathbf{R}_n(t,\tau)$ and $\mathbf{C}_n(t,\tau)$, defined by $\mathbf{R}_n(t,\tau) \stackrel{\text{def}}{=} \mathrm{E}[\mathbf{n}(t+\tau/2)\mathbf{n}^H(t-\tau/2)]$ and $\mathbf{C}_n(t,\tau) \stackrel{\text{def}}{=} \mathrm{E}[\mathbf{n}(t+\tau/2)\mathbf{n}^T(t-\tau/2)]$. Using (1), it is easy to verify that $\mathbf{R}_n(t,\tau)$ and $\mathbf{C}_n(t,\tau)$ are periodic functions of t, whose periods are equal to T and T, respectively for R signals, and to T and $2T$, respectively for QR signals. Matrices $\mathbf{R}_n(t,\tau)$ and $\mathbf{C}_n(t,\tau)$ have then Fourier series expansions given by

$$\mathbf{R}_n(t,\tau) = \sum_{\alpha_i} \mathbf{R}_n^{\alpha_i}(\tau) e^{j2\pi\alpha_i t} \quad (4)$$

$$\mathbf{C}_n(t,\tau) = \sum_{\beta_i} \mathbf{C}_n^{\beta_i}(\tau) e^{j2\pi\beta_i t}. \quad (5)$$

Here, α_i and β_i are the so-called non-conjugate and conjugate SO cyclic frequencies of $\mathbf{n}(t)$, such that $\alpha_i = i/T$ $(i \in \mathbb{Z})$ for both R and QR signals, whereas $\beta_i = i/T$ and $\beta_i = (2i+1)/2T$ $(i \in \mathbb{Z})$ for R and QR signals, respectively [39], [40], $\mathbf{R}_n^{\alpha_i}(\tau)$ and $\mathbf{C}_n^{\beta_i}(\tau)$ are the first and second cyclic correlation matrices of $\mathbf{n}(t)$ for the cyclic frequencies α_i and β_i and the delay τ, defined by

$$\mathbf{R}_n^{\alpha_i}(\tau) \stackrel{\text{def}}{=} < \mathbf{R}_n(t,\tau) e^{-j2\pi\alpha_i t} > \quad (6)$$

$$\mathbf{C}_n^{\beta_i}(\tau) \stackrel{\text{def}}{=} < \mathbf{C}_n(t,\tau) e^{-j2\pi\beta_i t} >, \quad (7)$$

where $< . >$ is the temporal mean operation in t over an infinite observation duration. Note that (6) and (7) for $\alpha_i = \beta_i = 0$ simply reduce to $< \mathbf{R}_n(t,\tau) >$ and $< \mathbf{C}_n(t,\tau) >$, respectively. The Fourier transforms $\mathbf{R}_n^{\alpha_i}(f)$ and $\mathbf{C}_n^{\beta_i}(f)$, of $\mathbf{R}_n^{\alpha_i}(\tau)$ and $\mathbf{C}_n^{\beta_i}(\tau)$, respectively, are called the first and second cyclospectrum of $\mathbf{n}(t)$ for the cyclic frequencies α_i and β_i, respectively.

B. Two-input extended models for standard WL processing

For both R and QR signals, a conventional linear processing of $\mathbf{x}(t)$ only exploits the information contained at the zero non-conjugate $(\alpha = 0)$ SO cyclic frequency of $\mathbf{x}(t)$, through the exploitation of the temporal mean $< \mathbf{R}_x(t,\tau) >$ of the first correlation matrix, $\mathbf{R}_x(t,\tau) \stackrel{\text{def}}{=} \mathrm{E}[\mathbf{x}(t+\tau/2)\mathbf{x}^H(t-\tau/2)]$, of $\mathbf{x}(t)$. It does not exploit the potential SO non-circularity of $\mathbf{x}(t)$.

For R signals, a standard WL or two-input processing of $\mathbf{x}(t)$, only exploits the information contained at the zero non-conjugate and conjugate $(\alpha_0, \beta_0) = (0,0)$ SO cyclic frequencies of $\mathbf{x}(t)$ through the exploitation of the temporal mean $< \mathbf{R}_{\tilde{x}}(t,\tau) >$ of the first correlation matrix $\mathbf{R}_{\tilde{x}}(t,\tau) \stackrel{\text{def}}{=} \mathrm{E}[\widetilde{\mathbf{x}}(t+\tau/2)\widetilde{\mathbf{x}}^H(t-\tau/2)]$, of the two-input extended model $\widetilde{\mathbf{x}}(t) \stackrel{\text{def}}{=} [\mathbf{x}^T(t), \mathbf{x}^H(t)]^T$, defined by

$$\widetilde{\mathbf{x}}(t) = \sum_\ell \widetilde{\mathbf{G}}(t\text{–}\ell T)\mathbf{b}_\ell + \widetilde{\boldsymbol{\epsilon}}(t) = \sum_\ell b_\ell \widetilde{\mathbf{g}}(t\text{–}\ell T) + \widetilde{\mathbf{n}}(t), \quad (8)$$

where $\widetilde{\boldsymbol{\epsilon}}(t) \stackrel{\text{def}}{=} [\boldsymbol{\epsilon}^T(t), \boldsymbol{\epsilon}^H(t)]^T$, $\widetilde{\mathbf{n}}(t) \stackrel{\text{def}}{=} [\mathbf{n}^T(t), \mathbf{n}^H(t)]^T$, $\widetilde{\mathbf{G}}(t) \stackrel{\text{def}}{=} [\widetilde{\mathbf{g}}(t), \widetilde{\mathbf{g}}_1(t), .., \widetilde{\mathbf{g}}_P(t)]$, $\widetilde{\mathbf{g}}(t) \stackrel{\text{def}}{=} [\mathbf{g}^T(t), \mathbf{g}^H(t)]^T$, $\widetilde{\mathbf{g}}_p(t) \stackrel{\text{def}}{=} [\mathbf{g}_p^T(t), \mathbf{g}_p^H(t)]^T$, $1 \leq p \leq P$, and $\mathbf{b}_\ell \stackrel{\text{def}}{=} [b_\ell, b_{1,\ell}, ...b_{P,\ell}]^T$. Note that $< \mathbf{R}_{\tilde{x}}(t,\tau) >$ conveys the information contained in both $< \mathbf{R}_x(t,\tau) >$ and $< \mathbf{C}_x(t,\tau) >$ and thus exploits the potential SO non-circularity of $\mathbf{x}(t)$ when $(a_\ell, a_{p,\ell}) = (b_\ell, b_{p,\ell})$ in (1).

For QR signals, as no information is contained at $\beta = 0$, i.e., in $< \mathbf{C}_x(t,\tau) >$, when $(a_\ell, a_{p,\ell}) = (j^\ell b_\ell, j^\ell b_{p,\ell})$ in (1), a derotation preprocessing of the data is required

before standard WL filtering. Using (1) with $(a_\ell, a_{p,\ell}) = (j^\ell b_\ell, j^\ell b_{p,\ell})$ for QR signals, the derotated observation vector can be written as:

$$\begin{aligned}\mathbf{x}_d(t) &\stackrel{\text{def}}{=} j^{-t/T}\mathbf{x}(t) = \sum_\ell \mathbf{G}_d(t-\ell T)\mathbf{b}_\ell + \boldsymbol{\epsilon}_d(t) \\ &= \sum_\ell b_\ell \mathbf{g}_d(t-\ell T) + \mathbf{n}_d(t), \end{aligned} \quad (9)$$

where $\boldsymbol{\epsilon}_d(t) \stackrel{\text{def}}{=} j^{-t/T}\boldsymbol{\epsilon}(t)$, $\mathbf{n}_d(t) \stackrel{\text{def}}{=} j^{-t/T}\mathbf{n}(t)$, $\mathbf{G}_d(t) \stackrel{\text{def}}{=} [\mathbf{g}_d(t), \mathbf{g}_{1,d}(t), .., \mathbf{g}_{P,d}(t)] = v_d(t) \otimes \mathbf{H}_d(t)$, $\mathbf{g}_d(t) \stackrel{\text{def}}{=} j^{-t/T}\mathbf{g}(t)$, $\mathbf{g}_{p,d}(t) \stackrel{\text{def}}{=} j^{-t/T}\mathbf{g}_p(t)$, $v_d(t) \stackrel{\text{def}}{=} j^{-t/T}v(t)$, $\mathbf{H}_d(t) \stackrel{\text{def}}{=} [\mathbf{h}_d(t), \mathbf{h}_{1,d}(t), .., \mathbf{h}_{P,d}(t)]$, $\mathbf{h}_d(t) \stackrel{\text{def}}{=} j^{-t/T}\mathbf{h}(t)$ and $\mathbf{h}_{p,d}(t) \stackrel{\text{def}}{=} j^{-t/T}\mathbf{h}_p(t)$. Note that the derotation operation of $\mathbf{x}(t)$ may also be defined, alternatively, as $\mathbf{x}_d(t) \stackrel{\text{def}}{=} j^{t/T}\mathbf{x}(t)$. Expression (9) shows that the derotation operation makes a QR signal looks like an R signal, with a non-zero information at the zero conjugate SO cyclic frequency. Indeed, it is easy to verify [33] that $\mathbf{x}_d(t)$ has non-conjugate, $\alpha_{d,i}$ and conjugate, $\beta_{d,i}$, SO cyclic frequencies such that $\alpha_{d,i} = \alpha_i = i/T$ and $\beta_{d,i} = \beta_i - 1/2T = i/T$, which proves the presence of information at $\beta_{d,0} = 0$. Thus standard WL or two-input processing of QR signals, exploits the information contained at $(\alpha_{d,0}, \beta_{d,0}) = (0,0)$ through the exploitation of the temporal mean $< \mathbf{R}_{\tilde{x}_d}(t,\tau) >$, of the first correlation matrix, $\mathbf{R}_{\tilde{x}_d}(t,\tau) \stackrel{\text{def}}{=} \mathrm{E}[\widetilde{\mathbf{x}}_d(t+\tau/2)\widetilde{\mathbf{x}}_d^H(t-\tau/2)]$, of the two-input extended derotated model $\widetilde{\mathbf{x}}_d(t) \stackrel{\text{def}}{=} [\mathbf{x}_d^T(t), \mathbf{x}_d^H(t)]^T$, defined by

$$\widetilde{\mathbf{x}}_d(t) = \sum_\ell \widetilde{\mathbf{G}}_d(t-\ell T)\mathbf{b}_\ell + \widetilde{\boldsymbol{\epsilon}}_d(t) = \sum_\ell b_\ell \widetilde{\mathbf{g}}_d(t-\ell T) + \widetilde{\mathbf{n}}_d(t), \quad (10)$$

where $\widetilde{\boldsymbol{\epsilon}}_d(t) \stackrel{\text{def}}{=} [\boldsymbol{\epsilon}_d^T(t), \boldsymbol{\epsilon}_d^H(t)]^T$, $\widetilde{\mathbf{n}}_d(t) \stackrel{\text{def}}{=} [\mathbf{n}_d^T(t), \mathbf{n}_d^H(t)]^T$, $\widetilde{\mathbf{G}}_d(t) \stackrel{\text{def}}{=} [\widetilde{\mathbf{g}}_d(t), \widetilde{\mathbf{g}}_{1,d}(t), .., \widetilde{\mathbf{g}}_{P,d}(t)]$, $\widetilde{\mathbf{g}}_d(t) \stackrel{\text{def}}{=} [\mathbf{g}_d^T(t), \mathbf{g}_d^H(t)]^T$ and $\widetilde{\mathbf{g}}_{p,d}(t) \stackrel{\text{def}}{=} [\mathbf{g}_{p,d}^T(t), \mathbf{g}_{p,d}^H(t)]^T$, $1 \le p \le P$. Note that $< \mathbf{R}_{\tilde{x}_d}(t,\tau) >$ conveys the information contained in both $< \mathbf{R}_{x_d}(t,\tau) \stackrel{\text{def}}{=} \mathrm{E}[\mathbf{x}_d(t+\tau/2)\mathbf{x}_d^H(t-\tau/2)] >$ and $< \mathbf{C}_{x_d}(t,\tau) \stackrel{\text{def}}{=} \mathrm{E}[\mathbf{x}_d(t+\tau/2)\mathbf{x}_d^T(t-\tau/2)] >$ and thus exploits the potential SO non-circularity of $\mathbf{x}_d(t)$. This is equivalent to exploit the energy contained in the SO cyclic frequencies $(\alpha_0, \beta_0) = (0, 1/2T)$ of $\mathbf{x}(t)$.

C. Three-input extended models for WL FRESH processing

C1) *Sub-optimality of the two-input model and interest of a M-input model with $M > 2$:* The two-input model introduced in the previous section exploits the information contained in the SO cyclic frequencies $(\alpha_0, \beta_0) = (0,0)$ of $\mathbf{x}(t)$ for R signals and in $(\alpha_{d,0}, \beta_{d,0}) = (0,0)$ of $\mathbf{x}_d(t)$, or equivalently in $(\alpha_0, \beta_0) = (0, 1/2T)$ of $\mathbf{x}(t)$, for QR signals.

For R signals/MUI, a large amount of energy is contained in the SO cyclic frequencies $(\alpha_0, \beta_0) = (0,0)$, whatever the real-valued filter $v(t)$, and this energy is equally distributed in α_0 and β_0. Moreover, the energy contained in $\alpha_i = \beta_i = i/T$, $i \neq 0$, increases with the signals/MUI bandwidth and decreases with an increasing value of $|i|$ [35], [39]. Consequently, for small signals/MUI bandwidth, the SO cyclic energy of R signals/MUI is mainly contained in $(\alpha_0, \beta_0) = (0,0)$, the energy contained in $\alpha_i = \beta_i = i/T$, $i \neq 0$ is negligible and the two-input model (8) is SO quasi-optimal. However, for increasing signals/MUI bandwidth, the SO cyclic energy contained in $\alpha_1 = \beta_1 = 1/T$ and in $\alpha_{-1} = \beta_{-1} = -1/T$ is equally distributed and is no longer negligible with respect to that on (α_0, β_0). In this case, the two-input model becomes sub-optimal and it may be useful to built M-input models ($M > 2$) able to fetch the energy contained in the latter non-zero SO cyclic frequencies of the observations to improve the performance of receivers. Note that increasing again the number of input to fetch the energy contained in $\alpha_i = \beta_i = i/T$ for $|i| > 1$ is generally useless since only a very weak residual energy is contained in these non-zero SO cyclic frequencies.

For QR signals/MUI, a large amount of energy is contained in the SO cyclic frequencies $(\alpha_0, \beta_0, \beta_{-1}) = (0, 1/2T, -1/2T)$ of $\mathbf{x}(t)$, or, equivalently, in $(\alpha_{d,0}, \beta_{d,0}, \beta_{d,-1}) = (0,0,-1/T)$ of $\mathbf{x}_d(t)$, with an equal energy on β_0, β_{-1}, $\beta_{d,0}$ and $\beta_{d,-1}$ [40], whatever the real-valued filter $v(t)$. Consequently, the two-input model (10), which only exploits the SO energy contained in $(\alpha_{d,0}, \beta_{d,0}) = (0,0)$, i.e., a part of the main energy, is sub-optimal whatever the bandwidth $B > 1/(2T)$, for which the energy contained in β_0, β_{-1}, $\beta_{d,0}$ and $\beta_{d,-1}$ is not zero. It may then be useful to built M-input models ($M > 2$) able to fetch, at least, the energy contained in $(\alpha_{d,0}, \beta_{d,0}, \beta_{d,-1}) = (0,0,-1/T)$. As the SO cyclic energy contained in $\alpha_{d,i} = i/T$ ($i \neq 0$) and in $\beta_{d,i} = i/T$ ($i \neq 0$ and $i \neq -1$) increases with the signals/MUI bandwidth, the sub-optimality of the two-input model (10) increases with the signals/MUI bandwidth. Finally, note that a further increase of the number of input to fetch the energy contained in $\alpha_{d,i}$ for $|i| > 1$ and in $\beta_{d,i}$ for $i \neq 0$ and $i \neq -1$ is generally useless since these energies are generally negligible with respect to the one contained in $\alpha_{d,0}$, $\beta_{d,0}$ and $\beta_{d,-1}$.

C2) *Three-input FRESH model:* To fetch most of the residual SO cyclic energy which is not exploited by the two-input models (8) and (10), for R and QR signals respectively, well-suited M-input models ($M > 2$) must be built. It will be shown in the following of the paper that a three-input FRESH model is generally sufficient to fetch most of the SO cyclic energy which is not used by the two-input model. Moreover, a three-input model is a good compromise between performance and complexity of the implementation.

For R signals, we propose the three-input FRESH model defined by

$$\mathbf{x}_3(t) \stackrel{\text{def}}{=} [\mathbf{x}^T(t), \mathbf{x}^H(t), e^{-j2\pi t/T}\mathbf{x}^H(t)]^T, \quad (11)$$

whereas for QR signals, we propose the following three-input model

$$\begin{aligned}\mathbf{x}_3(t) &\stackrel{\text{def}}{=} [\mathbf{x}_d^T(t), \mathbf{x}_d^H(t), e^{-j2\pi t/T}\mathbf{x}_d^H(t)]^T \\ &= j^{-t/T}[\mathbf{x}^T(t), e^{j2\pi t/2T}\mathbf{x}^H(t), e^{-j2\pi t/2T}\mathbf{x}^H(t)]^T \\ &\stackrel{\text{def}}{=} j^{-t/T}\mathbf{x}_3'(t). \end{aligned} \quad (12)$$

A three-input processing of $\mathbf{x}(t)$ exploits the temporal mean, $< \mathbf{R}_{x_3}(t,\tau) >$, of the first correlation matrix, $\mathbf{R}_{x_3}(t,\tau) \stackrel{\text{def}}{=} \mathrm{E}[\mathbf{x}_3(t+\tau/2)\mathbf{x}_3^H(t-\tau/2)]$, of $\mathbf{x}_3(t)$. Using (6) and (7) and developing $< \mathbf{R}_{x_3}(t,\tau) >$, it is straightforward to verify that $< \mathbf{R}_{x_3}(t,\tau) >$ exploits the information contained in $(\alpha_0, \alpha_{-1}, \alpha_1, \beta_0, \beta_{-1}) = (0, -1/T, 1/T, 0, -1/T)$ for R signals and in $(\alpha_0, \alpha_{-1}, \alpha_1, \beta_{d,0}, \beta_{d,-1}) = (0, -1/T, 1/T, 0, -1/T)$ for QR signals, which corresponds, in this latter case, to $(\alpha_0, \alpha_{-1}, \alpha_1, \beta_0, \beta_{-1}) = (0, -1/T, 1/T, 1/2T, -1/2T)$. Following the analysis of the previous section, we deduce that, whatever the pulse shaping filter, the three-input model (11) for R signals exploits all the main non-conjugate and conjugate energetical SO cyclic frequencies of $\mathbf{x}(t)$, except β_1, whereas the three-input model (12) for QR signals exploits all the main non-conjugate and conjugate energetical SO cyclic frequencies of $\mathbf{x}(t)$. Note that a time invariant linear processing of $\mathbf{x}_3(t)$ becomes now a time varying WL processing of $\mathbf{x}(t)$, called here three-input WL FRESH processing of $\mathbf{x}(t)$.

Note that, for R signals, the three-input model (11) might also be defined by $\mathbf{x}_3(t) = [\mathbf{x}^T(t), \mathbf{x}^H(t), e^{j2\pi t/T}\mathbf{x}^H(t)]^T$ For QR signals, the three-input model $\mathbf{x}_3'(t)$ might have also been chosen instead of $\mathbf{x}_3(t)$, which has been done in [33]. An alternative three-input model for QR signals might also be defined by $\mathbf{x}_3(t) = [\mathbf{x}_d^T(t), \mathbf{x}_d^H(t), e^{j2\pi t/T}\mathbf{x}_d^H(t)]^T$ provided that $\mathbf{x}_d(t)$ is, in this case, defined by $\mathbf{x}_d(t) \stackrel{\text{def}}{=} j^{t/T}\mathbf{x}(t)$.

D. M-input generic model for L, standard WL and WL FRESH processing

In the following, we consider L, standard WL and WL FRESH MMSE receivers as one, two and three-input receivers respectively. Then, for the M-input MMSE receivers $(M = 1, 2, 3)$, we denote by $\mathbf{x}_M(t)$ the generic observation vector. For linear receivers $(M = 1)$, $\mathbf{x}_M(t)$ reduces to $\mathbf{x}(t)$ for R signals and to $\mathbf{x}_d(t)$ for QR signals. For standard WL or two-input receivers $(M = 2)$, $\mathbf{x}_M(t)$ corresponds to $\widetilde{\mathbf{x}}(t)$ for R signals and to $\widetilde{\mathbf{x}}_d(t)$ for QR signals. For WL FRESH or three-input receivers $(M = 3)$, $\mathbf{x}_M(t)$ corresponds to $\mathbf{x}_3(t)$ defined by (11) and (12) for R and QR signals respectively. We then deduce from (1) and (8) to (12) that $\mathbf{x}_M(t)$ always takes the form

$$\begin{aligned}\mathbf{x}_M(t) &= \sum_\ell b_\ell \mathbf{g}_M(t-\ell T) + \sum_{1\le p\le P}\sum_\ell b_{p,\ell}\mathbf{g}_{p,M}(t-\ell T) + \boldsymbol{\epsilon}_M(t) \\ &= \sum_\ell \mathbf{G}_M(t-\ell T)\mathbf{b}_\ell + \boldsymbol{\epsilon}_M(t) \\ &\stackrel{\text{def}}{=} \sum_\ell b_\ell \mathbf{g}_M(t-\ell T) + \mathbf{n}_M(t). \end{aligned} \quad (13)$$

Here, $\mathbf{g}_M(t)$, $\mathbf{g}_{p,M}(t)$, $\boldsymbol{\epsilon}_M(t)$ and $\mathbf{n}_M(t)$ are defined in a similar way as $\mathbf{x}_M(t)$, where $\mathbf{x}(t)$ is replaced by $\mathbf{g}(t)$, $\mathbf{g}_p(t)$, $\boldsymbol{\epsilon}(t)$ and $\mathbf{n}(t)$, respectively, whereas $\mathbf{G}_1(t) = \mathbf{G}(t)$ for R signals and $\mathbf{G}_1(t) = \mathbf{G}_d(t)$ for QR signals, $\mathbf{G}_2(t) = \widetilde{\mathbf{G}}(t)$ for R signals and $\mathbf{G}_2(t) = \widetilde{\mathbf{G}}_d(t)$ for QR signals, whereas matrix $\mathbf{G}_3(t)$ is defined by $\mathbf{G}_3(t) \stackrel{\text{def}}{=} [\mathbf{g}_3(t), \mathbf{g}_{1,3}(t), ..., \mathbf{g}_{P,3}(t)]$.

III. M-INPUT MMSE RECEIVERS

In this section we compute, for R and QR signals, M-input MMSE receivers $(M = 1, 2, 3)$, both with and without the structure constraint, fully exploiting or not the MUI waveform knowledge.

A. MMSE criterion

As for R and QR signals, $a_n = b_n$ and $a_n = j^n b_n$ respectively, where b_n are real-valued zero-mean independent random variables, an M-input MMSE receiver considered in this paper generates an output $\mathbf{y}_M(t)$ which minimizes, at each symbol time nT, the MSE criterion defined by

$$\mathrm{MSE} = \mathrm{E}(|b_n - y_M(nT)|^2). \quad (14)$$

Note that the MSE is here minimized at each symbol time contrary to the MSE considered in [35] which is minimized at every moment t. In other words, the approach considered in this paper is an equalization approach, whereas the one considered in [35] is a signal estimation approach. The different M-input receivers considered in the paper differ in their structure and the assumptions made about the MUI.

B. One and two-input MMSE receivers with a particular structure constraint

B1) *Presentation:* In order to simplify their implementation, most of the L and WL MMSE receivers of the literature are computed at the symbol rate after a matched filtering operation to the pulse shaping filter. They have thus a particular structure constraint, which is shown in this paper to be generally sub-optimal in most cases. These L and WL receivers are called in the following sc M-input MMSE receivers with $M = 1$ and 2, respectively. To compute the sc M-input MMSE receiver, we denote by $\mathbf{x}_v(t) \stackrel{\text{def}}{=} v^*(-t) \otimes \mathbf{x}(t)$, the observation vector after matched filtering operation to the pulse-shaping filter. We then deduce

from (1) and (13) that, after the sampling operation at the symbol rate, the M-input observation vector becomes,

$$\begin{aligned}\mathbf{x}_{v,M}(nT) &= \sum_{\ell} b_\ell \mathbf{g}_{v,M}((n-\ell)T) \\ &+ \sum_{1\le p\le P}\sum_{\ell} b_{p,\ell}\mathbf{g}_{p_{v,M}}((n-\ell)T)+\boldsymbol{\epsilon}_{v,M}(nT) \\ &= \sum_{\ell}\mathbf{G}_{v,M}((n-\ell)T)\mathbf{b}_\ell + \boldsymbol{\epsilon}_{v,M}(nT) \\ &\stackrel{\text{def}}{=} \sum_{\ell} b_\ell \mathbf{g}_{v,M}((n-\ell)T) + \mathbf{n}_{v,M}(nT). \quad (15)\end{aligned}$$

Here, $\mathbf{x}_{v,M}(t)$, $\mathbf{g}_{v,M}(t)$, $\mathbf{g}_{p_{v,M}}(t)$, $\boldsymbol{\epsilon}_{v,M}(t)$ and $\mathbf{n}_{v,M}(t)$ are defined in a similar way as $\mathbf{x}_M(t)$, where $\mathbf{x}(t)$ is replaced by $\mathbf{x}_v(t)$, $\mathbf{g}_v(t)$, $\mathbf{g}_{p_v}(t)$, $\boldsymbol{\epsilon}_v(t)$ and $\mathbf{n}_v(t)$ respectively, with $\mathbf{a}_v(t) \stackrel{\text{def}}{=} v^*(-t)\otimes\mathbf{a}(t)$, whereas $\mathbf{G}_{v,M}(t)$ is defined in a similar way as $\mathbf{G}_M(t)$ where $\mathbf{g}_v(t)$ and $\mathbf{g}_{p_v}(t)$ replace $\mathbf{g}(t)$ and $\mathbf{g}_p(t)$, respectively. We denote by ${\mathbf{w}_M^d}^*(-kT)$, the samples of the discrete time (DT) M-input receiver whose output at time nT is defined by

$$y_M(nT) = \sum_k {\mathbf{w}_M^d}^H(-kT)\mathbf{x}_{v,M}((n-k)T). \quad (16)$$

Note that the d-index is used in the paper to characterize either DT quantities or Fourier transform of DT quantities and that ${\mathbf{w}_M^d}^*(-kT)$ has the dimension $MN\times 1$. The DT M-input receiver, ${\mathbf{w}_M^d}^*(-kT)$, whose output (16) minimizes (14) is denoted by ${\mathbf{w}_{M_{sc}}^d}^*(-kT)$ and is called sc M-input MMSE receiver. It is proved in Appendix A that the frequency response, ${\mathbf{w}_{M_{sc}}^d}^*(f)$, of ${\mathbf{w}_{M_{sc}}^d}^*(-kT)$ is such that:

$$\begin{aligned}\mathbf{w}_{M_{sc}}^d(f) &= \pi_b[\mathbf{R}_{x_{v,M}}^d(f)]^{-1}\mathbf{g}_{v,M}^d(f) \\ &= \Big[1/\pi_b + {\mathbf{g}_{v,M}^d}^H(f)[\mathbf{R}_{n_{v,M}}^d(f)]^{-1}\mathbf{g}_{v,M}^d(f)\Big]^{-1} \\ &\qquad [\mathbf{R}_{n_{v,M}}^d(f)]^{-1}\mathbf{g}_{v,M}^d(f) \\ &\stackrel{\text{def}}{=} c_{M_{sc}}^d(f)[\mathbf{R}_{n_{v,M}}^d(f)]^{-1}\mathbf{g}_{v,M}^d(f), \quad (17)\end{aligned}$$

if $v(f)$ does not vanish in $[-1/2T, +1/2T]$. Otherwise $\mathbf{w}_{M_{sc}}^d(f) = \mathbf{0}$ for the frequencies f which are outside the support of $\mathbf{g}_{v,M}^d(f)$, i.e., such that $\mathbf{x}_{v,M}^d(f) = \mathbf{0}$, where $\mathbf{x}_{v,M}^d(f)$ is the Fourier transform of $\mathbf{x}_{v,M}(nT)$. Here $\pi_b \stackrel{\text{def}}{=} \mathrm{E}(b_k^2)$, $c_{M_{sc}}^d(f)$ and $\mathbf{g}_{v,M}^d(f)$, both periodic of period $1/T$, are the inverse scalar term appearing in (17) and the frequency response of the DT SOI channel vector $\mathbf{g}_{v,M}(kT)$, respectively, such that

$$\mathbf{g}_{v,M}^d(f) = \sum_k \mathbf{g}_{v,M}(kT)e^{-j2\pi fkT} = \frac{1}{T}\sum_{\ell}\mathbf{g}_{v,M}(f-\frac{\ell}{T}). \quad (18)$$

Matrices $\mathbf{R}_{x_{v,M}}^d(f)$ and $\mathbf{R}_{n_{v,M}}^d(f)$ are the Fourier transforms of matrices $\mathbf{R}_{x_{v,M}}^d(kT) \stackrel{\text{def}}{=} \mathrm{E}[\mathbf{x}_{v,M}(nT)\mathbf{x}_{v,M}^H((n-k)T)]$ and $\mathbf{R}_{n_{v,M}}^d(kT) \stackrel{\text{def}}{=} \mathrm{E}[\mathbf{n}_{v,M}(nT)\mathbf{n}_{v,M}^H((n-k)T)]$, respectively, where the DT vectors $\mathbf{x}_{v,M}(nT)$ and $\mathbf{n}_{v,M}(nT)$ are SO stationary, defined by

$$\begin{aligned}\mathbf{R}_{x_{v,M}}^d(f) &= \sum_k \mathbf{R}_{x_{v,M}}^d(kT)e^{-j2\pi fkT} \\ &= \mathbf{R}_{n_{v,M}}^d(f) + \pi_b\mathbf{g}_{v,M}^d(f){\mathbf{g}_{v,M}^d}^H(f). \quad (19) \\ \mathbf{R}_{n_{v,M}}^d(f) &= \sum_k \mathbf{R}_{n_{v,M}}^d(kT)e^{-j2\pi fkT} \\ &= \sum_{p=1}^P \pi_b\mathbf{g}_{p_{v,M}}^d(f){\mathbf{g}_{p_{v,M}}^d}^H(f) + \mathbf{R}_{\epsilon_{v,M}}^d(f) \quad (20)\end{aligned}$$

Here $\mathbf{g}_{p_{v,M}}^d(f)$ is defined similarly as $\mathbf{g}_{v,M}^d(f)$, where $\mathbf{g}_{v,M}(kT)$ is replaced by $\mathbf{g}_{p_{v,M}}(kT)$, and $\mathbf{R}_{\epsilon_{v,M}}^d(f)$ is the Fourier Transform of $\mathbf{R}_{\epsilon_{v,M}}^d(kT) \stackrel{\text{def}}{=} \mathrm{E}[\boldsymbol{\epsilon}_{v,M}(nT)\boldsymbol{\epsilon}_{v,M}^H((n-k)T)]$, defined by

$$\mathbf{R}_{\epsilon_{v,M}}^d(f) = \sum_k \mathbf{R}_{\epsilon_{v,M}}^d(kT)e^{-j2\pi fkT} = \frac{1}{T}\sum_{\ell}\mathbf{R}_{\epsilon_{v,M}}(f-\frac{\ell}{T}), \quad (21)$$

where $\mathbf{R}_{\epsilon_{v,M}}(f)$ is the Fourier transform of $\mathbf{R}_{\epsilon_{v,M}}(\tau) \stackrel{\text{def}}{=} \mathrm{E}[\boldsymbol{\epsilon}_{v,M}(t+\tau/2)\boldsymbol{\epsilon}_{v,M}^H(t-\tau/2)]$, since $\boldsymbol{\epsilon}_{v,M}(t)$ is SO stationary. Note that the second equality of (17) comes from the application of the Woodbury Identity to $[\mathbf{R}_{x_{v,M}}^d(f)]^{-1}$, using (19). The output, at time kT, of the sc M-input MMSE receiver is given by

$$\begin{aligned}y_{M_{sc}}(k) &= T\int_\Delta {\mathbf{w}_{M_{sc}}^d}^H(f)\mathbf{x}_{v,M}^d(f)e^{j2\pi fkT}df \\ &= \int {\mathbf{w}_{M_{sc}}^d}^H(f)\mathbf{x}_{v,M}(f)e^{j2\pi fkT}df \\ &= T\int_\Delta c_{M_{sc}}^d(f){\mathbf{g}_{v,M}^d}^H(f)[\mathbf{R}_{n_{v,M}}^d(f)]^{-1}\mathbf{x}_{v,M}^d(f)e^{j2\pi fkT}df \\ &= \int c_{M_{sc}}^d(f){\mathbf{g}_{v,M}^d}^H(f)[\mathbf{R}_{n_{v,M}}^d(f)]^{-1}\mathbf{x}_{v,M}(f)e^{j2\pi fkT}df \quad (22)\end{aligned}$$

where $\Delta \stackrel{\text{def}}{=} [-1/2T, 1/2T]$. Note that when $v(f)$ vanishes in Δ, the integration appearing in (22) is over the frequency support of $\mathbf{x}_{v,M}^d(f)$ or $\mathbf{x}_{v,M}(f)$. Expressions (17) and (22) show that, for both R and QR signals, sub-optimal L and WL MMSE receivers with the structure constraint of the literature, are composed of two operations, as depicted in Fig.1. The first one, ${\mathbf{g}_{v,M}^d}^H(f)[\mathbf{R}_{n_{v,M}}^d(f)]^{-1}$, implements a DT M-input spatio-temporal or spatio-frequential matched filter to the global channel of the SOI in a spatially and temporally colored total noise, which is stationary in this case. The second one, $c_{M_{sc}}^d(f)$, implements a scalar digital filtering operation, corresponding to an MMSE equalizer of the SOI channel at the output of the matched filter. Note that the implementation of the receivers (17) requires the a priori knowledge or estimation of $\mathbf{R}_{x_{v,M}}^d(f)$ and $\mathbf{g}_{v,M}^d(f)$ and then of $\mathbf{h}(kT)$, i.e,. of the DT impulse response of the SOI channel vector only. Comparing (17) to (30), we find that $\mathbf{w}_{M_{sc}}^d(f)$ and $\mathbf{w}_{M_s}(f)$, both exploiting a true and false SO stationarity property of the MUI respectively, have very similar forms but where the matched filter to the SOI global

channel in colored noise is CT in (30) and DT in (17), at the symbol rate.

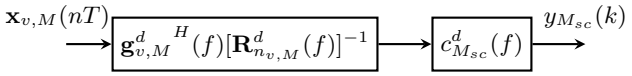

Fig. 1. Structure of the sc M-input MMSE receiver

B2) *Equivalence with the sc MMSE receivers jointly estimating the SOI and MUI symbols:* We show in this section that (17) also corresponds to the first column of the sc M-input MMSE receiver jointly estimating the SOI and MUI symbols, which fully exploit the MUI waveform. Denoting by $\mathbf{G}^d_{v,M}(f)$ the Fourier transform of $\mathbf{G}_{v,M}(kT)$, it is proved in Appendix A that (17) can also be written as

$$\begin{aligned}\mathbf{w}^d_{M_{sc}}(f) &= \pi_b[\mathbf{R}^d_{x_{v,M}}(f)]^{-1}\mathbf{G}^d_{v,M}(f)\mathbf{f} \\ &= [\mathbf{R}^d_{\epsilon_{v,M}}(f)]^{-1}\mathbf{G}^d_{v,M}(f)\{(1/\pi_b)\mathbf{I}_{P+1} \\ &+\mathbf{G}^d_{v,M}{}^H(f)[\mathbf{R}^d_{\epsilon_{v,M}}(f)]^{-1}\mathbf{G}^d_{v,M}(f)\}^{-1}\mathbf{f}, \quad (23)\end{aligned}$$

where $\mathbf{f}$ is the $(P+1)\times 1$ vector defined by $\mathbf{f} = [1,0,...,0]^T$. We then deduce from this result that the DT filter, $\mathbf{w}^d_{M_{sc}}{}^*(-kT)$, whose output at time nT (16) minimizes the MSE (14), also corresponds to the first column of the DT matrix, $\mathbf{W}^d_M{}^*(-kT)$, denoted by $\mathbf{W}^d_{M_{sc}}{}^*(-kT)$, whose output vector at time nT, $\mathbf{y}_M(nT) = \sum_k \mathbf{W}^d_M{}^H(-kT)\mathbf{x}_{v,M}((n-k)T)$, minimizes the joint MSE, JMSE $\stackrel{\text{def}}{=} \mathrm{E}[|\mathbf{b}_n - \mathbf{y}_M(n)|^2]$, where $\mathbf{b}_n$ has been defined in Section II-B. This result proves that with the previous structure constraint, expressions (23) and (17) are equivalent, which discards the need to know the MUI channels to implement the sc M-input MMSE receiver.

C. Optimal one and two-input MMSE receivers

To show the sub-optimality of the sc M-input MMSE receiver ($M = 1, 2$) for R and QR signals, it is necessary to compute the optimal M-input MMSE receiver ($M = 1, 2$), called o M-input MMSE receiver in the following. Contrary to the sc M-input MMSE receiver, the o M-input MMSE receiver has no structure constraint and fully exploit the waveform of the MUI, which means that it takes into account the explicit MUI form appearing in model (1). This implicitly consists to take into account the cyclostationarity of the MUI, for $M = 1, 2$, in addition to their SO non-circularity, for $M = 2$. We denote by $\mathbf{w}^*_M(-t)$, the CT M-input receiver whose output is defined by

$$y_M(t) = \mathbf{w}^H_M(-t) \otimes \mathbf{x}_M(t). \quad (24)$$

Note that $\mathbf{w}^*_M(-t)$ has the dimension $MN \times 1$. The CT M-input receiver, $\mathbf{w}^*_M(-t)$, whose output (24) minimizes (14) at each symbol time, is denoted by $\mathbf{w}^*_{M_o}(-t)$ and is called optimal or o M-input MMSE receiver. It is proved in Appendix B that the frequency response, $\mathbf{w}^*_{M_o}(f)$, of $\mathbf{w}^*_{M_o}(-t)$ is such that

$$\begin{aligned}\mathbf{w}_{M_o}(f) &= \mathbf{G}_M(f)[(N_0/\pi_b)\mathbf{I}_{P+1} \\ &+ 1/T\sum_\ell \mathbf{G}^H_M(f-\ell/T)\mathbf{G}_M(f-\ell/T)]^{-1}\mathbf{f} \\ &\stackrel{\text{def}}{=} \mathbf{G}_M(f)\mathbf{C}^d_{M_o}(f)\mathbf{f} \stackrel{\text{def}}{=} \mathbf{G}_M(f)\mathbf{c}^d_{M_o}(f). \quad (25)\end{aligned}$$

Here N_0 is the power spectral density of each component of the noise vector $\boldsymbol{\epsilon}(t)$, $\mathbf{f}$ has been defined after (23), $\mathbf{C}^d_{M_0}(f)$ is the $(P+1)\times(P+1)$ inverse matrix appearing in (25), which is periodic of period $1/T$, whereas $\mathbf{c}^d_{M_0}(f) \stackrel{\text{def}}{=} \mathbf{C}^d_{M_0}(f)\mathbf{f}$ is a $(P+1)\times 1$ vector. We deduce from (25) that $\mathbf{w}^*_{M_o}(-t)$ also corresponds to the first column of the matrix $\mathbf{W}^*_M(-t)$, of dimension $MN \times (P+1)$, denoted by $\mathbf{W}^*_{M_o}(-t)$, whose output vector, $\mathbf{y}_M(t) = \mathbf{W}^H_M(-t)\otimes\mathbf{x}_M(t)$, minimizes, at each symbol time, the joint MSE criterion, JMSE $\stackrel{\text{def}}{=} \mathrm{E}[|\mathbf{b}_n - \mathbf{y}_M(n)|^2]$. Hence, once the waveform of the MUI is fully exploited, estimating the SOI symbols only or jointly with the MUI symbols give rise to two equivalent approaches for the SOI symbols estimation.

Furthermore, it is important to note, which is proved in Appendix B, that, for both R and QR signals, the optimal three-input WL MMSE receiver whose input is $\mathbf{x}_3(t)$, is the receiver whose frequency response, $\mathbf{w}^*_{3_o}(f)$, is given by

$$\mathbf{w}^*_{3_o}(f) = [\mathbf{w}^H_{2_o}(f), \mathbf{0}^T]^T, \quad (26)$$

where $\mathbf{w}_{2_o}(f)$ is given by (25) for $M = 2$. This confirms that the o two-input MMSE receiver optimally exploits all the SO cyclostationarity of the MUI.

The output, at time kT, of the o M-input MMSE receiver is given

$$\begin{aligned}y_{M_0}(k) &= \int \mathbf{w}^H_{M_0}(f)\mathbf{x}_M(f)e^{j2\pi fkT}df \\ &= \int \mathbf{c}^d_{M_o}{}^H(f)\mathbf{G}^H_M(f)\mathbf{x}_M(f)e^{j2\pi fkT}df, \quad (27)\end{aligned}$$

To make $\mathbf{c}^d_{M_o}(f)$ more concrete, we compute its expression in the presence of $P = 1$ MUI, which gives in this case $\mathbf{c}^d_{M_o}(f) = [c^d_{M,1}(f), c^d_{M,2}(f)]^T$, where $c^d_{M,1}(f)$ and $c^d_{M,2}(f)$ are given by

$$c^d_{M,1}(f) = \frac{\pi_b(N_0 + \frac{\pi_b}{T}\sum_\ell \|\mathbf{g}_{1,M}(f-\frac{\ell}{T})\|^2)}{\begin{cases}(N_0+\frac{\pi_b}{T}\sum_\ell \|\mathbf{g}_M(f-\frac{\ell}{T})\|^2) \\ \qquad (N_0+\frac{\pi_b}{T}\sum_\ell \|\mathbf{g}_{1,M}(f-\frac{\ell}{T})\|^2) \\ -\frac{\pi_b^2}{T^2}|\sum_\ell \mathbf{g}^H_M(f-\frac{\ell}{T})\mathbf{g}_{1,M}(f-\frac{\ell}{T})|^2\end{cases}} \quad (28)$$

$$c^d_{M,2}(f) = \frac{-\frac{\pi_b^2}{T}\sum_\ell \mathbf{g}^H_{1,M}(f-\frac{\ell}{T})\mathbf{g}_M(f-\frac{\ell}{T})}{\begin{cases}(N_0+\frac{\pi_b}{T}\sum_\ell \|\mathbf{g}_M(f-\frac{\ell}{T})\|^2) \\ \qquad (N_0+\frac{\pi_b}{T}\sum_\ell \|\mathbf{g}_{1,M}(f-\frac{\ell}{T})\|^2) \\ -\frac{\pi_b^2}{T^2}|\sum_\ell \mathbf{g}^H_M(f-\frac{\ell}{T})\mathbf{g}_{1,M}(f-\frac{\ell}{T})|^2\end{cases}} \quad (29)$$

where $\mathbf{G}_M(f) \stackrel{\text{def}}{=} [\mathbf{g}_M,(f), \mathbf{g}_{1,M}(f)]$. Expressions (25) and (27) show that, for both R and QR signals, optimal L and

WL MMSE receivers are composed of three operations, as depicted in Fig.2. The first one, $\mathbf{G}_M^H(f)$, implements a set of $P+1$ CT matched filtering operation to the global channels of SOI and MUI. The second one is a sampling, to the symbol rate, of each of these matched filter outputs. The third one, ${\mathbf{c}_{M_o}^d}^H(f)$, implements a set of $P+1$ discrete-time (TD) or digital filtering operations, applied to the previous $P+1$ sampled outputs, which performs the SOI channel equalization jointly with the noise plus MUI minimization. Note that the implementation of the receivers (25) requires the a priori knowledge or estimation of N_0 and $\mathbf{G}(t)$, and then of $\mathbf{H}(t)$, i.e., of the impulse response of both the SOI and MUI channel vectors, which may be cumbersome for a practical implementation.

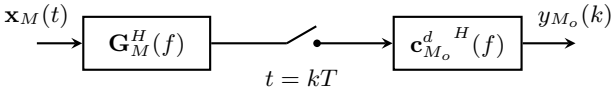

Fig. 2. Structure of the o M-input MMSE receiver

D. One, two and three input MMSE receivers falsely assuming SO stationary MUI

One way to build, for R and QR signals, M-input MMSE receivers ($M = 1, 2, 3$) discarding the need to know or to estimate the MUI channels without inserting any structure constraint, is to estimate the SOI symbols only, assuming that the MUI are falsely SO stationary. We denote by $\mathbf{w}_M^*(-t)$, the CT M-input receiver whose output is defined by (24). The CT M-input receiver, $\mathbf{w}_M^*(-t)$, whose output (24) minimizes (14) at each symbol time, assuming that the MUI, and then the total noise $\mathbf{n}_M(t)$ in (13), are falsely SO stationary, is denoted by $\mathbf{w}_{M_s}^*(-t)$ and is called s M-input MMSE receiver. It is proved in AppendixC that the frequency response, $\mathbf{w}_{M_s}^*(f)$, of $\mathbf{w}_{M_s}^*(-t)$ is such that

$$\begin{aligned}\mathbf{w}_{M_s}(f) &= \Big\{(1/\pi_b) + (1/T)\sum_{\ell} \mathbf{g}_M^H(f-\ell/T) \\ &[\mathbf{R}_{n,M}^0(f-\ell/T)]^{-1}\mathbf{g}_M(f-\ell/T)\Big\}^{-1}[\mathbf{R}_{n_M}^0(f)]^{-1}\mathbf{g}_M(f) \\ &\stackrel{\text{def}}{=} c_{M_s}^d(f)[\mathbf{R}_{n_M}^0(f)]^{-1}\mathbf{g}_M(f). \qquad (30)\end{aligned}$$

Here, $c_{M_s}^d(f)$ is the inverse scalar term appearing in (30), which is periodic of period $1/T$, $\mathbf{g}_1(f) = \mathbf{g}(f)$ for R signals and $\mathbf{g}_1(f) = \mathbf{g}_d(f)$ for QR signals, $\mathbf{g}_2(f) = \widetilde{\mathbf{g}}(f)$ for R signals and $\mathbf{g}_2(f) = \widetilde{\mathbf{g}}_d(f)$ for QR signals, $\mathbf{g}_3(f) \stackrel{\text{def}}{=} [\mathbf{g}^T(f), \mathbf{g}^H(-f), \mathbf{g}^H(-1/T-f)]^T$ for R signals and $\mathbf{g}_3(f) \stackrel{\text{def}}{=} [\mathbf{g}_d^T(f), \mathbf{g}_d^H(-f), \mathbf{g}_d^H(-1/T-f)]^T = [\mathbf{g}^T(f+1/4T), \mathbf{g}^H(1/4T-f), \mathbf{g}^H(-3/4T-f)]^T$ for QR signals, $\mathbf{R}_{n_M}^0(f)$ defined as the Fourier transform of $\mathbf{R}_{n_M}^0(\tau) \stackrel{\text{def}}{=} < \mathrm{E}[\mathbf{n}_M(t+\tau/2)\mathbf{n}_M^H(t-\tau/2)] >$ corresponds to the power spectral density matrix of $\mathbf{n}_M(t)$. Using (1), it is easy to verify that $\mathbf{R}_{n_M}^0(f)$ is given by

$$\begin{aligned}\mathbf{R}_{n_M}^0(f) &= \frac{\pi_b}{T}\sum_{1\le p\le P}\mathbf{g}_{p,M}(f)\mathbf{g}_{p,M}^H(f) + N_0\mathbf{I}_{NM} \\ &= \mathbf{R}_{x_M}^0(f) - \frac{\pi_b}{T}\mathbf{g}_M(f)\mathbf{g}_M^H(f), \qquad (31)\end{aligned}$$

where $\mathbf{g}_{p,M}(f)$ is defined in a similar way as $\mathbf{g}_M(f)$ but where $\mathbf{g}(f)$ is replaced by $\mathbf{g}_p(f)$ and where $\mathbf{R}_{x_M}^0(f)$ is the power spectral density matrix of $\mathbf{x}_M(t)$, defined in a similar way as $\mathbf{R}_{n_M}^0(f)$, with $\mathbf{x}_M(t)$ instead of $\mathbf{n}_M(t)$. The output, at time kT, of the s M-input MMSE receiver is given by

$$\begin{aligned}y_{M_s}(k) &= \int \mathbf{w}_{M_s}^H(f)\mathbf{x}_M(f)e^{j2\pi fkT}df \\ &= \int c_{M_s}^d(f)\mathbf{g}_M^H(f)[\mathbf{R}_{n_M}^0(f)]^{-1}\mathbf{x}_M(f)e^{j2\pi fkT}df \qquad (32)\end{aligned}$$

Expressions (30) and (32) show that, for both R and QR signals, sub-optimal L and WL MMSE receivers without any structure constraint falsely assuming SO stationary MUI, are composed of three operations, as depicted in Fig.3. The first one, $\mathbf{g}_M^H(f)[\mathbf{R}_{n_M}^0(f)]^{-1}$, implements a CT M-input spatio-temporal or spatio-frequential pseudo-matched filter to the global channel of the SOI in a spatially and temporally colored total noise. The second operation is a sampling, to the symbol rate, of this pseudo-matched filter output. The third one, $c_{M_s}^d(f)$, implements a scalar digital filtering operation, corresponding to a pseudo-MMSE equalizer of the SOI channel at the output of the pseudo-matched filter. Note that the implementation of the receivers (30) requires the a priori knowledge or estimation of $\mathbf{R}_n^0(f)$ and $\mathbf{g}(t)$, and then of $\mathbf{h}(t)$, i.e., of the impulse response of the SOI channel vector only, discarding the need to estimate the MUI channel vectors, which may be advantageous for a practical implementation.

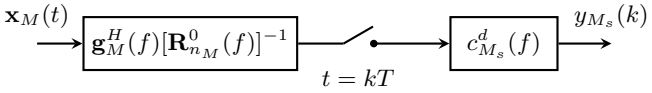

Fig. 3. Structure of the s M-input MMSE receiver

E. Particular case of an absence of MUI

In the absence of MUI and for $M = 1, 2$, the total noise is SO stationary and thus the s M-input MMSE receivers and the o M-input MMSE receivers coincide. In this case, $\mathbf{G}_M(f)$, $\mathbf{R}_{n,M}(f)$ and $\mathbf{R}_{n_{v,M}}^d(f)$ reduce to $\mathbf{g}_M(f)$, $\mathbf{R}_{\epsilon,M}(f) = N_0\mathbf{I}_{NM}$ and $\mathbf{R}_{\epsilon_{v,M}}^d(f)$, respectively, and we deduce from (17), (25) and (30) that:

$$\begin{aligned}\mathbf{w}_{M_o}(f) &= \mathbf{w}_{M_s}(f) = \\ &\{(N_0/\pi_b) + (1/T)\sum_{\ell}\|\mathbf{g}_M(f-\ell/T)\|^2\}^{-1}\mathbf{g}_M(f) \qquad (33)\end{aligned}$$

$$\begin{aligned}\mathbf{w}_{M_{sc}}^d(f) = \{1/\pi_b + {\mathbf{g}_{v,M}^d}^H(f)[\mathbf{R}_{\epsilon_{v,M}}^d(f)]^{-1}\mathbf{g}_{v,M}^d(f)\}^{-1} \\ [\mathbf{R}_{\epsilon_{v,M}}^d(f)]^{-1}\mathbf{g}_{v,M}^d(f). \qquad (34)\end{aligned}$$

Inserting (33) in (27) and (34) in (22), it is straightforward to show that in the general case of a frequency selective SOI channel, $y_{M_{sc}}(k)$ and $y_{M_o}(k)$ are generally different, which shows the sub-optimality of sc M-input MMSE receivers, and thus of most of L and WL MMSE receivers of the literature. Nevertheless, a more detailed analysis of $y_{M_{sc}}(k)$ and $y_{M_o}(k)$ allows us to prove the equality of $y_{M_{sc}}(k)$, $y_{M_s}(k)$ and $y_{M_o}(k)$, and thus the optimality of (34), if one of the two following conditions is verified

$$\text{(a)} \quad \mathbf{h}(f) = \mathbf{h} \tag{35}$$

$$\text{(b)} \quad \text{The bandwidth of } v(t) \text{ is included in } \Delta. \tag{36}$$

Note that condition (b) is verified for OQAM constellations.

IV. SINR AT THE OUTPUT OF THE M-INPUT MMSE RECEIVERS

In this section, we compute the general expression of the SINR at the output of a M-input MMSE receiver before decision.

A. Generic output of the M-input MMSE receiver before decision

We deduce from (22), (27) and (32) that the generic output of the M-input MMSE receivers considered in this paper can be written as

$$y_{M_g}(k) = \int \mathbf{w}_{M_g}^H(f)\mathbf{x}_{M_g}(f)e^{j2\pi fkT}df \tag{37}$$

where it is easy to verify from (13) and (15) that

$$\mathbf{x}_{M_g}(f) = \sum_{\ell} b_l e^{-j2\pi f\ell T}\mathbf{g}_{M_g}(f) + \mathbf{n}_{M_g}(f). \tag{38}$$

Note that $(y_{M_g}(k), \mathbf{w}_{M_g}(f), \mathbf{x}_{M_g}(f), \mathbf{g}_{M_g}(f), \mathbf{n}_{M_g}(f)) = (y_{M_{sc}}(k), \mathbf{w}^d_{M_{sc}}(f), \mathbf{x}_{v_M}(f), \mathbf{g}_{v_M}(f), \mathbf{n}_{v_M}(f))$, $(y_{M_g}(k), \mathbf{w}_{M_g}(f), \mathbf{x}_{M_g}(f), \mathbf{g}_{M_g}(f), \mathbf{n}_{M_g}(f)) = (y_{M_o}(k), \mathbf{w}_{M_o}(f), \mathbf{x}_M(f), \mathbf{g}_M(f), \mathbf{n}_M(f))$, $(y_{M_g}(k), \mathbf{w}_{M_g}(f), \mathbf{x}_{M_g}(f), \mathbf{g}_{M_g}(f), \mathbf{n}_{M_g}(f)) = (y_{M_s}(k), \mathbf{w}_{M_s}(f), \mathbf{x}_M(f), \mathbf{g}_M(f), \mathbf{n}_M(f))$ for the receivers of Sections III-B, III-C and III-D, respectively. Inserting (38) into (37), we obtain:

$$\begin{aligned} y_{M_g}(k) &= b_k \int \mathbf{w}_{M_g}^H(f)\mathbf{g}_{M_g}(f)df \\ &+ \sum_{\ell\neq k} b_\ell \int \mathbf{w}_{M_g}^H(f)\mathbf{g}_{M_g}(f)e^{j2\pi f(k-\ell)T}df \\ &+ \int \mathbf{w}_{M_g}^H(f)\mathbf{n}_{M_g}(f)e^{j2\pi fkT}df \stackrel{\text{def}}{=} b_k u_{M_g} + e_{M_g}(k), \end{aligned} \tag{39}$$

where it is easy to verify that u_{M_g} is a real-valued quantity and where $e_{M_g}(k)$ is the contribution of the Intersymbol Interference (ISI), the MUI and the background noise in $y_{M_g}(k)$. As b_k is a real-valued symbol, it is well-known that, assuming a circular Gaussian $e_{M_g}(k)$, a conventional ML receiver whose input is (39), decides the symbols from the real-part of $y_{M_g}(k)$, given by

$$z_{M_g}(k) \stackrel{\text{def}}{=} \mathrm{Re}(y_{M_g}(k)) = b_k u_{M_g} + \mathrm{Re}(e_{M_g}(k)). \tag{40}$$

B. Generic SINR at the output of the M-input MMSE receiver before decision

The SER at the output of the generic receiver $\mathbf{w}_{M_g}^H(f)$ is directly linked to the SINR in $z_{M_g}(k)$, denoted by $\mathrm{SINR}_{M_g}(k)$. Using the fact that the quantities $b_k u_{M_g}$ and $\mathrm{Re}(e_{M_g}(k))$ are uncorrelated, we deduce that $\mathrm{SINR}_{M_g}(k)$ can be written as

$$\begin{aligned} \mathrm{SINR}_{M_g}(k) &= \frac{\pi_b u_{M_g}^2}{\mathrm{E}[(\mathrm{Re}(e_{M_g}(k)))^2]} \\ &= \frac{2\pi_b u_{M_g}^2}{\mathrm{E}[|y_{M_g}^2(k)|] + \mathrm{Re}(\mathrm{E}[y_{M_g}^2(k)]) - 2\pi_b u_{M_g}^2}. \end{aligned} \tag{41}$$

In the presence of R or QR MUI, the CT output $y_{M_g}(t)$ is SO cyclostationary, which implies that $\mathrm{E}[|y_{M_g}^2(k)|]$ and $\mathrm{E}[y_{M_g}^2(k)]$ have Fourier series expansions given by [33].

$$\mathrm{E}[|y_{M_g}^2(k)|] = \sum_{\gamma_i} e^{j2\pi\gamma_i kT} \int r_{y_{M_g}}^{\gamma_i}(f)df \tag{42}$$

$$\mathrm{E}[y_{M_g}^2(k)] = \sum_{\delta_i} e^{j2\pi\delta_i kT} \int c_{y_{M_g}}^{\delta_i}(f)df. \tag{43}$$

Here, the quantities γ_i and δ_i denote the non-conjugate and conjugate SO cyclic frequencies of $y_{M_g}(t)$, respectively, whereas $r_{y_{M_g}}^{\gamma_i}(f)$ and $c_{y_{M_g}}^{\delta_i}(f)$ are the Fourier transforms of the first, $r_{y_{M_g}}^{\gamma_i}(\tau)$, and second, $c_{y_{M_g}}^{\delta_i}(\tau)$, cyclic correlation functions of $y_{M_g}(t)$ for the delay τ and the cyclic frequencies γ_i and δ_i, respectively. Moreover, as $y_{M_g}(t)$ is the output of the filter $\mathbf{w}_{M_g}^H(f)$ whose input is $\mathbf{x}_{M_g}(t)$, we can write

$$r_{y_{M_g}}^{\gamma_i}(f) = \mathbf{w}_{M_g}^H(f+\gamma_i/2)\mathbf{R}_{x_{M_g}}^{\gamma_i}(f)\mathbf{w}_{M_g}(f-\gamma_i/2) \tag{44}$$

$$c_{y_{M_g}}^{\delta_i}(f) = \mathbf{w}_{M_g}^H(f+\delta_i/2)\mathbf{C}_{x_{M_g}}^{\delta_i}(f)\mathbf{w}_{M_g}^*(\delta_i/2-f), \tag{45}$$

where $\mathbf{R}_{x_{M_g}}^{\gamma_i}(f)$ and $\mathbf{C}_{x_{M_g}}^{\delta_i}(f)$ are the Fourier transforms of the first, $\mathbf{R}_{x_{M_g}}^{\gamma_i}(\tau)$, and second, $\mathbf{C}_{x_{M_g}}^{\delta_i}(\tau)$, cyclic correlation matrices of $\mathbf{x}_{M_g}(t)$ for the delay τ and the cyclic frequency γ_i and δ_i respectively. In the presence of MUI having same nature (R or QR), symbol period and carrier frequency as the SOI, it is straightforward to verify that for all the previous considered receivers ($M = 1, 2, 3$; R and QR signals), $\gamma_i = \delta_i = \alpha_i = i/T$, $i \in \mathbb{Z}$. This implies that (42) (43) and then, $\mathrm{SINR}_{M_g}(k)$, do not depend on k and $\mathrm{SINR}_{M_g}(k)$ is simply denoted by SINR_{M_g}. Using (39) and (42) to (45) into (41),

we obtain:

$$\mathrm{SINR}_{M_g} = \frac{2\pi_b u_{M_g}^2}{\left\{\begin{array}{l}\sum_{\alpha_i}\int[\mathbf{w}_{M_g}^H(f+\alpha_i/2)\mathbf{R}_{x_{M_g}}^{\alpha_i}(f)\mathbf{w}_{M_g}(f-\alpha_i/2)\\ +\mathrm{Re}(\mathbf{w}_{M_g}^H(f+\alpha_i/2)\mathbf{C}_{x_{M_g}}^{\alpha_i}(f)\mathbf{w}_{M_g}^*(\alpha_i/2-f))]df\end{array}\right.-2\pi_b u_{M_g}^2} \quad (46)$$

where $u_{M_g} \stackrel{\mathrm{def}}{=} \int \mathbf{w}_{M_g}^H(f)\mathbf{g}_{M_g}(f)df$. As for $M=2$, it is straightforward to prove that $y_{M_g}(k)$ is real-valued whatever the considered receiver, SINR_{2_g} reduces in this case to:

$$\mathrm{SINR}_{2_g} = \frac{\pi_b[\int \mathbf{w}_{2_g}^H(f)\mathbf{g}_{2_g}(f)df]^2}{\left\{\begin{array}{c}\sum_{\alpha_i}\int \mathbf{w}_{2_g}^H(f+\alpha_i/2)\mathbf{R}_{x_{2_g}}^{\alpha_i}(f)\mathbf{w}_{2_g}(f-\alpha_i/2)df\\ -\pi_b[\int \mathbf{w}_{2_g}^H(f)\mathbf{g}_{2_g}(f)df]^2\end{array}\right.}. \quad (47)$$

For the sc and o MMSE receivers, simple specific closed-forms expressions of the SINR are useful to numerically calculate (46) and (47).

For the sc M-input MMSE receiver ($M=1,2$), as $\mathbf{x}_{v,M}(nT)$ (15) and $y_{M_{sc}}(k)$ (22) are SO stationary, it is proved in Appendix A that (46) and (47) can be written as

$$\mathrm{SINR}_{M_{sc}} = \frac{2\pi_b T[\int_\Delta \mathbf{g}_{v,M}^{d^H}(f)[\mathbf{R}_{x_{v,M}}^d(f)]^{-1}\mathbf{g}_{v,M}^d(f)df]^2}{\left\{\begin{array}{l}\int_\Delta \mathbf{g}_{v,M}^{d^H}(f)[\mathbf{R}_{x_{v,M}}^d(f)]^{-1}\mathbf{g}_{v,M}^d(f)df\\ +\mathrm{Re}[\int_\Delta \mathbf{g}_{v,M}^{d^H}(f)[\mathbf{R}_{x_{v,M}}^d(f)]^{-1}\mathbf{C}_{x_{v,M}}^d(f)[\mathbf{R}_{x_{v,M}}^{d^*}(-f)]^{-1}\\ \mathbf{g}_{v,M}^{d^*}(-f)df]-2\pi_b T[\int_\Delta \mathbf{g}_{v,M}^{d^H}(f)[\mathbf{R}_{x_{v,M}}^d(f)]^{-1}\mathbf{g}_{v,M}^d(f)df]^2\end{array}\right.} \quad (48)$$

$$\mathrm{SINR}_{2_{sc}} = \frac{\pi_b T\int_\Delta \mathbf{g}_{v,2}^{d^H}(f)[\mathbf{R}_{x_{v,2}}^d(f)]^{-1}\mathbf{g}_{v,2}^d(f)df}{1-\pi_b T\int_\Delta \mathbf{g}_{v,2}^{d^H}(f)[\mathbf{R}_{x_{v,2}}^d(f)]^{-1}\mathbf{g}_{v,2}^d(f)df}, \quad (49)$$

when $v(f)\neq 0$ in Δ which ensures that $\mathbf{R}_{x_{v,M}}^d(f)$ is not singular in Δ.

For the o M-input MMSE receiver ($M=1,2$), it is proved in Appendix B that (46) and (47) can be written as a function of the only matrix $\mathbf{C}_M^d(f)$ and vector $\mathbf{f}$ defined after (25), which gives

$$\mathrm{SINR}_{M_o} = \frac{2\pi_b[1-\frac{N_0T}{\pi_b}\int_\Delta \mathbf{f}^T\mathbf{C}_{M_o}^d(f)\mathbf{f}df]^2}{\left\{\begin{array}{l}N_0T\int_\Delta \mathbf{f}^T\mathbf{C}_{M_o}^d(f)\mathbf{f}df-\frac{2(N_0T)^2}{\pi_b}(\int_\Delta \mathbf{f}^T\mathbf{C}_{M_o}^d(f)\mathbf{f}df)^2\\ +\frac{N_0^2T}{\pi_b}\int_\Delta \mathrm{Re}[\mathbf{f}^T\mathbf{C}_{M_o}^d(f)\mathbf{C}_{M_o}^{d^*}(-f)\mathbf{f}]df\\ +\delta(M-2)[N_0T\int_\Delta \mathbf{f}^T\mathbf{C}_{M_o}^d(f)\mathbf{f}df\\ -\frac{N_0^2T}{\pi_b}\int_\Delta \mathbf{f}^T\mathbf{C}_{M_o}^d(f)\mathbf{C}_{M_o}^d(f)\mathbf{f}df]\end{array}\right.} \quad (50)$$

$$\mathrm{SINR}_{2_o} = \frac{\pi_b}{N_0T\int_\Delta \mathbf{f}^T\mathbf{C}_{2_o}^d(f)\mathbf{f}df}-1. \quad (51)$$

C. Total noise model and SO statistics

We assume in this section that the total noise $\mathbf{n}(t)$ is composed of a background noise and, at most, one MUI, which generates the observation model (1) with $P=1$. In this context, the purpose of this section is to compute and compare the SINR at the output of the previous M-input MMSE receivers for both R and QR signals. From (1), for both R and QR signals, for the sc and o M-input MMSE receivers ($M=1,2$) and s M-input MMSE receivers ($M=1,2,3$), $\mathbf{R}_{x_{M_g}}^{\alpha_i}(f)$ and $\mathbf{C}_{x_{M_g}}^{\alpha_i}(f)$ appearing in (46) can be written, from [33], as

$$\begin{aligned}\mathbf{R}_{x_{M_g}}^{\alpha_i}(f) &= \frac{\pi_b}{T}[\mathbf{g}_{M_g}(f+\alpha_i/2)\mathbf{g}_{M_g}^H(f-\alpha_i/2)\\ &\quad +\mathbf{g}_{1,M_g}(f+\alpha_i/2)\mathbf{g}_{1,M_g}^H(f-\alpha_i/2)]+\mathbf{R}_{\epsilon_{M_g}}^{\alpha_i}(f) \quad (52)\\ \mathbf{C}_{x_{M_g}}^{\alpha_i}(f) &= \frac{\pi_b}{T}[\mathbf{g}_{M_g}(f+\alpha_i/2)\mathbf{g}_{M_g}^T(\alpha_i/2-f)\\ &\quad +\mathbf{g}_{1,M_g}(f+\alpha_i/2)\mathbf{g}_{1,M_g}^T(\alpha_i/2-f)]+\mathbf{C}_{\epsilon_{M_g}}^{\alpha_i}(f) \quad (53)\end{aligned}$$

Here, $\mathbf{g}_{1,M_g}(f)=\mathbf{g}_{1,M}(f)$ for $g=o$ and ($M=1,2$) or $g=s$ and ($M=1,2,3$), where $\mathbf{g}_{1,3}(f) \stackrel{\mathrm{def}}{=} [\mathbf{g}_1^T(f),\mathbf{g}_1^H(-f),\mathbf{g}_1^H(-1/T-f)]^T$ for R signals, whereas $\mathbf{g}_{1,3}(f) \stackrel{\mathrm{def}}{=} [\mathbf{g}_{1,d}^T(f),\mathbf{g}_{1,d}^H(-f),\mathbf{g}_{1,d}^H(-1/T-f)]^T = [\mathbf{g}_1^T(f+1/4T),\mathbf{g}_1^H(1/4T-f),\mathbf{g}_1^H(-3/4T-f)]^T$ for QR signals. Besides, $\mathbf{g}_{1,M_g}(f)=\mathbf{g}_{1,v_M}(f)$ for $g=sc$ and ($M=1,2$). Moreover, $\mathbf{R}_{\epsilon_{M_g}}^{\alpha_i}(f)$ and $\mathbf{C}_{\epsilon_{M_g}}^{\alpha_i}(f)$ are such that:

$$\mathbf{R}_{\epsilon_{M_o}}^{\alpha_i}(f)=\mathbf{R}_{\epsilon_{M_s}}^{\alpha_i}(f)=N_0\delta(\alpha_i)\mathbf{I}_{MN}; \text{for } M=1,2 \quad (54)$$

$$\begin{aligned}\mathbf{R}_{\epsilon_{3_s}}^{\alpha_i}(f) &= N_0\delta(\alpha_i)\mathbf{I}_{3N}+N_0\delta(\alpha_i+1/T)\mathbf{J}_1^T\\ &\quad + N_0\delta(\alpha_i-1/T)\mathbf{J}_1 \quad (55)\\ \mathbf{R}_{\epsilon_{M_{sc}}}^{\alpha_i}(f) &= N_0|v(f)|^2\delta(\alpha_i)\mathbf{I}_{MN}; \text{for R signals,}\\ &\quad \text{for R signals and } M=1,2 \quad (56)\\ \mathbf{R}_{\epsilon_{M_{sc}}}^{\alpha_i}(f) &= N_0|v(f+1/4T)|^2\delta(\alpha_i)\mathbf{I}_N;\\ &\quad \text{for QR signals and } M=1 \quad (57)\end{aligned}$$

$$\mathbf{R}_{\epsilon_{M_{sc}}}^{\alpha_i}(f)=N_0\delta(\alpha_i)\begin{pmatrix}|v(f+1/4T)|^2\mathbf{I}_N & \mathbf{0}_N\\ \mathbf{0}_N & |v(-f+1/4T)|^2\mathbf{I}_N\end{pmatrix}; \text{for QR signals and } M=2 \quad (58)$$

$$\begin{aligned}\mathbf{C}_{\epsilon_{M_o}}^{\alpha_i}(f) &= \mathbf{C}_{\epsilon_{M_s}}^{\alpha_i}(f)=N_0\delta(\alpha_i)\delta(M-2)\mathbf{J}_{2N};\\ &\quad \text{for } M=1,2 \quad (59)\\ \mathbf{C}_{\epsilon_{3_s}}^{\alpha_i}(f) &= N_0\delta(\alpha_i)\mathbf{J}_2+N_0\delta(\alpha_i+1/T)\mathbf{J}_3 \quad (60)\\ \mathbf{C}_{\epsilon_{M_{sc}}}^{\alpha_i}(f) &= N_0|v(f)|^2\delta(\alpha_i)\delta(M-2)\mathbf{J}_{2N};\\ &\quad \text{for R signals and } M=1,2 \quad (61)\\ \mathbf{C}_{\epsilon_{M_{sc}}}^{\alpha_i}(f) &= \mathbf{0}_N \text{ for QR signals and } M=1 \quad (62)\end{aligned}$$

$$\mathbf{C}_{\epsilon_{M_{sc}}}^{\alpha_i}(f)=N_0\delta(\alpha_i)\begin{pmatrix}\mathbf{0}_N & |v(f+1/4T)|^2\mathbf{I}_N\\ |v(-f+1/4T)|^2\mathbf{I}_N & \mathbf{0}_N\end{pmatrix}; \text{for QR signals and } M=2 \quad (63)$$

where $\mathbf{J}_1$, $\mathbf{J}_2$ and $\mathbf{J}_3$ are the $3N\times 3N$ matrices defined by

$$\mathbf{J}_1=\begin{pmatrix}\mathbf{0}&\mathbf{0}&\mathbf{0}\\ \mathbf{0}&\mathbf{0}&\mathbf{I}\\ \mathbf{0}&\mathbf{0}&\mathbf{0}\end{pmatrix},\ \mathbf{J}_2=\begin{pmatrix}\mathbf{0}&\mathbf{I}&\mathbf{0}\\ \mathbf{I}&\mathbf{0}&\mathbf{0}\\ \mathbf{0}&\mathbf{0}&\mathbf{0}\end{pmatrix},\ \mathbf{J}_3=\begin{pmatrix}\mathbf{0}&\mathbf{0}&\mathbf{I}\\ \mathbf{0}&\mathbf{0}&\mathbf{0}\\ \mathbf{I}&\mathbf{0}&\mathbf{0}\end{pmatrix} \quad (64)$$

and $\mathbf{J}_{2N}$ is the $2N\times 2N$ exchange matrix $\begin{pmatrix}\mathbf{0}&\mathbf{I}\\ \mathbf{I}&\mathbf{0}\end{pmatrix}$.

D. SINR analysis in the absence of interference

To get more insights into the comparative behavior of the sc and o M-input MMSE receivers ($M = 1, 2$) for R and QR signals, we assume in this section an absence of MUI interference and a two-tap frequency selective channel such that

$$\mathbf{h}(t) = \mu_1 \delta(t)\mathbf{h}_1 + \mu_2 \delta(t-\tau)\mathbf{h}_2. \quad (65)$$

Here μ_1 and μ_2 ($0 \leq \mu_2 \leq \mu_1$) control the amplitude of the first and second paths of the SOI respectively, τ is the delay between the two paths and $\mathbf{h}_1$ and $\mathbf{h}_2$, deterministic or random, with components $h_1(i)$ and $h_2(i)$, $i = 1, .., N$, respectively, and such that $\mathrm{E}|h_1^2(i)| = \mathrm{E}|h_2^2(i)| = 1$, correspond to the channel vectors of the two paths, respectively. Using (65) into (1), we deduce that the mean SOI symbol energy per antenna, E_s, can be written as

$$\begin{aligned} E_s &= \frac{\pi_b}{N}\int \mathrm{E}(\|\mathbf{g}^2(t)\|)dt \\ &= \pi_b\mu_1^2\left[1+\beta^2+2\beta\mathrm{Re}\left(\mathrm{E}\left(\mathbf{h}_1^H\mathbf{h}_2/N\right)\right)r_v(\tau)\right], \quad (66) \end{aligned}$$

where $\beta \stackrel{\text{def}}{=} \mu_2/\mu_1$ is the selectivity coefficient of the channel and $r_v(t) \stackrel{\text{def}}{=} v(t) \otimes v^*(-t)$. Denoting by $\alpha_{1,2} \stackrel{\text{def}}{=} \mathbf{h}_1^H\mathbf{h}_2/(\|\mathbf{h}_1\|\|\mathbf{h}_2\|)$ the spatial correlation coefficient between $\mathbf{h}_1$ and $\mathbf{h}_2$ and assuming that, in the random case, $\mathbf{h}_1$ and $\mathbf{h}_2$ are statistically independent, expression (66) becomes

$$\begin{aligned} E_s &= \pi_b\mu_1^2[1+\beta^2+2\beta\mathrm{Re}(\alpha_{1,2})r_v(\tau)]; \\ &\quad \text{in the deterministic case,} \quad (67) \\ &= \pi_b\mu_1^2(1+\beta^2); \text{ in the random case.} \quad (68) \end{aligned}$$

For a propagation channel with no delay spread ($\beta = 0$), for both $M = 1$ and $M = 2$, for both R and QR signals, as mentioned in (35), the three receivers o, s and sc are equivalent and the expected value, $\mathrm{E}[\mathrm{SINR}_{M_g}]$, of the SINR at the output of these receivers, SINR_{M_g}, which corresponds to SINR_{M_g} for deterministic channels, is maximal and given by

$$\mathrm{E}[\mathrm{SINR}_{M_g}] = \frac{2NE_s}{N_0} \stackrel{\text{def}}{=} 2\epsilon_s. \quad (69)$$

Moreover, for both $M = 1$ and $M = 2$, for both R and QR signals, the three receivers o, s and sc are also equivalent in the two following situations:

- for R, $\pi/2$-BPSK and $\pi/2$-ASK SOI and arbitrary propagation channel, when $v(t)$ is a square-root raised cosine filter with a zero roll-off, as stated by (36).
- for OQAM SOI, when $v(t)$ is a square-root raised cosine filter with an arbitrary roll-off, as stated by (36).

Excepted the two previous situations, for both $M = 1$ and $M = 2$, for both R and QR signals, the sc M-input MMSE receiver (34) becomes sub-optimal with respect to the o M-input MMSE receiver and it has been verified by computer simulations that this sub-optimality increases with the SOI bandwidth (and thus with the roll-off for raised-cosine filters), the channel selectivity β, the modulus, $\alpha \stackrel{\text{def}}{=} |\alpha_{1,2}|$, of the spatial correlation coefficient between $\mathbf{h}_1$ and $\mathbf{h}_2$. Besides, this sub-optimality is more pronounced for deterministic than for random channels. To quantify and illustrate this sub-optimality of the sc M-input MMSE receivers, we assume now that (τ, ϕ) where ϕ is the phase of $\alpha_{1,2}$, are r.v. uniformly distributed on $[0, 4T] \times [0, 2\pi]$. Under these assumptions, choosing $N = 1$ (and thus $\alpha = 1$) and ϵ_s = 10 dB, Figs.4 and 5 show, for R and $\pi/2$-ASK QR signals respectively, for $M = 1, 2$, $\omega = 1$, $\beta = 1$ and deterministic channels, the variations of the estimated complementary cumulative distribution function $\Pr[(\mathrm{SINR}_{M_g}/2\epsilon_s)\mathrm{dB} \geq x\mathrm{dB}] \stackrel{\text{def}}{=} P_{M_g}(x)$ as a function of x (dB). Note that the curves appearing in these figures have been obtained from 10^5 Monte Carlo simulations where SINR_{M_g} have been computed from (46) to (47).

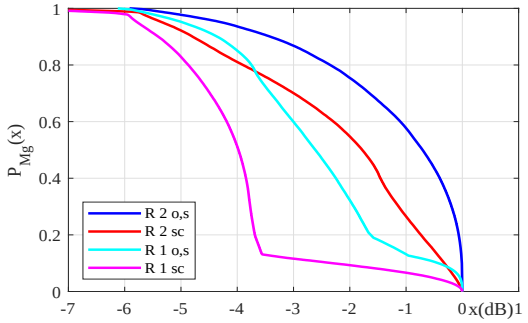

Fig. 4. $P_{M_g}(x)$ as a function of x ($N = 1$, $M = 1, 2$, $\epsilon_s = 10$ dB, $\omega = 1$, $\beta = 1$, deterministic channels, R signals.

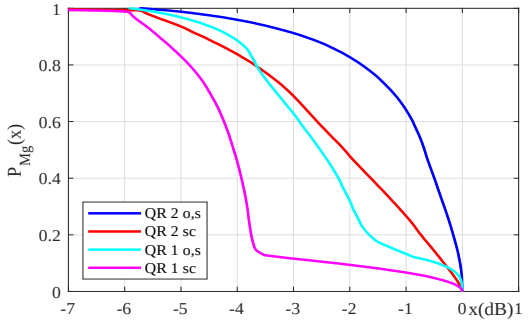

Fig. 5. $P_{M_g}(x)$ as a function of x ($N = 1$, $M = 1, 2$, $\epsilon_s = 10$ dB, $\omega = 1$, $\beta = 1$, deterministic channels, $\pi/2$-ASK QR signals.

We note the sub-optimality of the sc M-input MMSE receivers for both $M = 1, 2$ and for both R and QR signals. Note also the better performance of two-input receivers with respect to one-input ones due to the phase discrimination exploitation of the two paths. Note finally the similar performance for R and QR signals for $M = 1$ but, for $M = 2$, the slightly better performance of o receiver for QR signals. To complete these results, Figs.6 and 7 show the same variations as Figs.4 and 5 under the same assumptions but for Rayleigh fading channels for which $h_1(1)$ and $h_2(1)$

are i.i.d. random variables following a zero-mean circular Gaussian distribution. The conclusion of Figs.4 and 5 hold for Figs.6 and 7 with a lower sub-optimality of the sc receivers and similar performance of o receiver for R and QR signals.

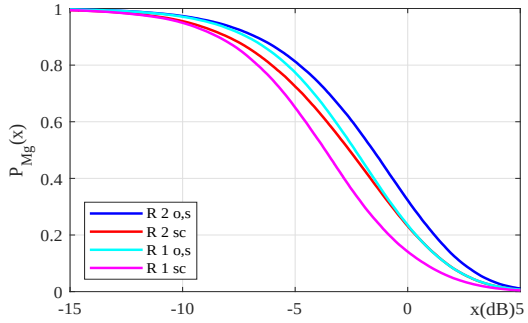

Fig. 6. $P_{M_g}(x)$ as a function of x ($N=1$, $M=1,2$, $\epsilon_s=10$ dB, $\omega=1$, $\beta=1$, Rayleigh channels, R signals.

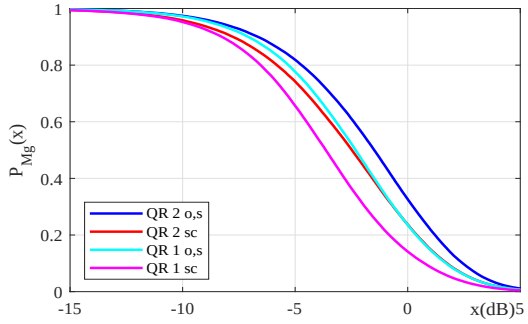

Fig. 7. $P_{M_g}(x)$ as a function of x ($N=1$, $M=1,2$, $\epsilon_s=10$ dB, $\omega=1$, $\beta=1$, Rayleigh channels, $\pi/2$-ASK QR signals.

Finally note that for $M=2$, interpretable closed-form expressions are possible when $\tau=\ell T$ where $\ell\in\mathbb{Z}^*$ in (65) where the SINR at the output of the o and s receivers for arbitrary roll-off are equal to the SINR at the output of the sc receiver for a zero roll-off, for which we get

$$\begin{aligned}\mathrm{SINR}_{R_{2,o}} &= \mathrm{SINR}_{R_{2,s}}=\mathrm{SINR}_{R_{2,sc}}\\ \mathrm{SINR}_{QR_{2,o}} &= \mathrm{SINR}_{QR_{2,s}}=\mathrm{SINR}_{QR_{2,sc}}\\ &=(1+2\epsilon_s)\left(\frac{1-\gamma^2}{1+\gamma^2}\right)-1 \text{ for } \beta\neq 0\\ &= 2\epsilon_s \qquad\qquad \text{for } \beta=0 \quad (70)\end{aligned}$$

where for $\beta\neq 0$:

$$\begin{aligned}\gamma &= \frac{(1+2\epsilon_s)(1+\beta^2)}{4\beta\epsilon_s\alpha\cos\phi}\left(1-\sqrt{1-\frac{16\beta^2\epsilon_s^2\alpha^2\cos^2\phi}{(1+2\epsilon_s)^2(1+\beta^2)^2}}\right)\\ &\qquad\qquad \text{for } \alpha\cos\phi\neq 0\\ &= 0 \qquad\qquad \text{for } \alpha\cos\phi=0 \quad (71)\end{aligned}$$

where $\phi=\mathrm{Arg}(\alpha_{1,2})$ and $\phi=\mathrm{Arg}(\alpha_{1,2})+\ell\pi/2$ for R and QR signals respectively. We clearly see that these SINR are decreasing when the spatial correlation α increases and that these SINR tend to $2\epsilon_s$ for β and $\alpha\cos\phi$ tending to zero for which γ tends to zero in (71).

E. SINR analysis for one MUI and channels with no delay spread

C1) *Propagation model:* To analyze the comparative behavior of the previous M-input MMSE receivers ($M=1,2,3$), for R and QR signals, in the presence of interference, we assume in this section the presence of one MUI and propagation channels with no delay spread such that

$$\mathbf{h}(t)=\mu\delta(t)\mathbf{h} \quad\text{and}\quad \mathbf{h}_1(t)=\mu_1\delta(t-\tau_1)\mathbf{h}_1. \qquad (72)$$

Here μ and μ_1 control the amplitude of the SOI and MUI respectively and τ_1 is the delay of the MUI with respect to the SOI. The vectors $\mathbf{h}$ and $\mathbf{h}_1$, random or deterministic, with components $h(i)$ and $h_1(i)$, $1\leq i\leq N$, respectively and such that $\mathrm{E}[|h(i)|^2]=\mathrm{E}[|h_1(i)|^2]=1$, $1\leq i\leq N$, correspond to the channel vectors of the SOI and MUI, respectively. Similarly as (67) and (68), the mean SOI and MUI energy per antenna, E_s and E_1 respectively are given by $E_s=\pi_b\mu^2$ and $E_1=\pi_{b_1}\mu_1^2$, where $\pi_{b_1}\overset{\text{def}}{=}\mathrm{E}(b_{1,k}^2)$. We then denote by ϵ_s and ϵ_1 the quantities $\epsilon_s\overset{\text{def}}{=}E_s\ \mathrm{E}(\|\mathbf{h}\|^2)/N_0=NE_s/N_0$ and $\epsilon_1\overset{\text{def}}{=}E_1\ \mathrm{E}(\|\mathbf{h}_1\|^2)/N_0=NE_1/N_0$.

C2) *Deterministic channels and SRRC filters (for T) with zero roll-off:* Under the previous assumptions, analytical interpretable expressions of SINR_{M_g} defined by (46) and (47) are only possible for a square root raised cosine (SRRC) filter $v(t)$ for the symbol duration T, i.e., for R, π/2-BPSK and π/2-ASK constellations with a zero roll-off $\omega=0$, which is assumed in this subsection. Otherwise, the computation of SINR_{M_g} can only be done numerically by computer simulations and will be discussed in the following subsections. Moreover, we assume in this subsection deterministic channels and we denote by $\alpha_{s,1}\overset{\text{def}}{=}|\alpha_{s,1}|e^{j\phi_{s,1}}$ the spatial correlation coefficient between the SOI and the MUI, such that $0\leq|\alpha_{s,1}|\leq 1$, and defined similarly as $\alpha_{1,2}$ by replacing $\mathbf{h}_1$ and $\mathbf{h}_2$ by $\mathbf{h}$ and $\mathbf{h}_1$, respectively. Finally, we denote by $\mathrm{SINR}_{R_{M_g}}$ and $\mathrm{SINR}_{QR_{M_g}}$ the SINR (46) at the output of the M-input MMSE receivers ($M=1,2,3$), for R and QR signals respectively.

a) *Case $|\alpha_{s,1}|\neq 1$*

When $|\alpha_{s,1}|\neq 1$, i.e., when there exists a spatial discrimination between the SOI and the MUI (which requires $N>1$), assuming a strong MUI ($\epsilon_1\gg 1$), we obtain from (46) and (47) after cumbersome derivations, the following

expressions:

$$\begin{aligned}\mathrm{SINR}_{R_{1,o}} &= \mathrm{SINR}_{R_{1,s}} = \mathrm{SINR}_{R_{1,sc}} \\ &\approx \mathrm{SINR}_{QR_{1,o}} = \mathrm{SINR}_{QR_{1,s}} = \mathrm{SINR}_{QR_{1,sc}} \\ &\approx 2\epsilon_s(1-|\alpha_{s,1}|^2) \quad (73)\\ \mathrm{SINR}_{R_{2,o}} &= \mathrm{SINR}_{R_{2,s}} = \mathrm{SINR}_{R_{2,sc}} \\ &\approx 2\epsilon_s(1-|\alpha_{s,1}|^2\cos^2\phi_{s,1}) \quad (74)\end{aligned}$$

$$\mathrm{SINR}_{QR_{2,o}} = \mathrm{SINR}_{QR_{2,sc}} \approx 2\epsilon_s\left(1-\frac{|\alpha_{s,1}|^2}{2}\right.$$
$$\left.\frac{(1+2\epsilon_s)(\cos^2\zeta_{s,1}+\cos^2\psi_{s,1})-4|\alpha_{s,1}|^2\epsilon_s\cos^2\zeta_{s,1}\cos^2\psi_{s,1}}{(1+2\epsilon_s)-|\alpha_{s,1}|^2\epsilon_s(\cos^2\zeta_{s,1}+\cos^2\psi_{s,1})}\right) \quad (75)$$

which reduces to (74) for synchronous SOI and MUI ($\tau_1 = 0$).

$$\mathrm{SINR}_{QR_{2,s}} \approx 2\epsilon_s\left(1-\frac{|\alpha_{s,1}|^2}{2}\right.$$
$$\left.\frac{1+\cos^2\psi_{s,1}+2\epsilon_s(1+\cos^2\psi_{s,1}(1-2|\alpha_{s,1}|^2))}{1+\epsilon_s(2-|\alpha_{s,1}|^2(1+\cos^2\psi_{s,1}))}\right), \quad (76)$$

After cumbersome derivations, whose some steps are given in Appendix D, it is proved that, for synchronous SOI and MUI ($\tau_1 = 0$), whatever the values of ϵ_s, ϵ_1 and $\alpha_{s,1}$, $\mathrm{SINR}_{R_{3,s}} = \mathrm{SINR}_{QR_{3,s}}$, showing equivalent performance of the s three-input MMSE receiver for R and QR signals, which is not the case for the s two-input MMSE receiver as shown in (74) and (76). For the general case of potentially asynchronous SOI and MUI, we deduce from the results of Appendix D, the following expressions:

$$\mathrm{SINR}_{R_{3,s}} \approx 2\epsilon_s\left(1-|\alpha_{s,1}|^2\right.$$
$$\left.\left(\frac{(1+8\cos^2\phi_{s,1})-|\alpha_{s,1}|^2(1+2\cos^2\phi_{s,1})^2}{9-|\alpha_{s,1}|^2(5+4\cos^2\phi_{s,1})}\right)\right) \quad (77)$$

$$\mathrm{SINR}_{QR_{3,s}} \approx 2\epsilon_s\left(1-|\alpha_{s,1}|^2\right.$$
$$\left.\left.\left(\frac{A(\epsilon_s,|\alpha_{s,1}|^2,\cos^2\psi_{s,1},\cos^2\zeta_{s,1})}{B(\epsilon_s,|\alpha_{s,1}|^2,\cos^2\psi_{s,1},\cos^2\zeta_{s,1})}\right)\right) \quad (78)$$

where A and B are second-order polynomial in ϵ_s, whereas $\psi_{s,1} \stackrel{\mathrm{def}}{=} \phi_{s,1} - \pi\tau_1/2T$ and $\zeta_{s,1} \stackrel{\mathrm{def}}{=} \phi_{s,1} + \pi\tau_1/2T$. We deduce from (74) to (76) that $\mathrm{SINR}_{R_{2,g}}/\epsilon_s$ does not depend on ϵ_s, while $\mathrm{SINR}_{QR_{2,g}}/\epsilon_s$ depends on ϵ_s, which proves the absence (for R signals) and the presence (for QR signals) of ISI in the output $z_{2_g}(k)$. Similarly, we deduce from (68) and (69) that $\mathrm{SINR}_{R_{3,s}}/\epsilon_s$ does not depend on ϵ_s while $\mathrm{SINR}_{QR_{3,s}}/\epsilon_s$ depends on ϵ_s, which proves the absence (for R signals) and the presence (for QR signals) of ISI in the output $z_{3_s}(k)$. Note that for $\epsilon_s \ll 1$, i.e., when the ISI becomes negligible with respect to the noise in $z_{3_s}(k)$, (78) reduces to

$$\mathrm{SINR}_{QR_{3,s}} \approx 2\epsilon_s\left(1-|\alpha_{s,1}|^2\right.$$
$$\left.\left(\frac{(1-|\alpha_{s,1}|^2)(1+\Gamma)^2+(2-\Gamma)\Gamma}{(1-|\alpha_{s,1}|^2)(5+2\Gamma)+2(2-\Gamma)}\right)\right);\ \epsilon_s \ll 1, \quad (79)$$

where $\Gamma \stackrel{\mathrm{def}}{=} \cos^2\psi_{s,1} + \cos^2\zeta_{s,1}$. For synchronous SOI and MUI, $\Gamma = 2\cos^2\phi_{s,1}$ and we verify that (77) and (79) give the same expressions.

b) *Case* $|\alpha_{s,1}| = 1$

When $|\alpha_{s,1}| = 1$, i.e., when there is no spatial discrimination between the SOI and the MUI, which is in particular the case for $N = 1$, after tedious computations, we obtain, for $M = 1$

$$\begin{aligned}\mathrm{SINR}_{R_{1,o}} &= \mathrm{SINR}_{R_{1,s}} = \mathrm{SINR}_{R_{1,sc}} \\ &= \frac{2\epsilon_s}{1+2\epsilon_1\cos^2\phi_{s,1}} \quad (80)\\ \mathrm{SINR}_{QR_{1,o}} &= \mathrm{SINR}_{QR_{1,s}} = \mathrm{SINR}_{QR_{1,sc}} \\ &= \frac{2\epsilon_s}{1+\epsilon_1(\cos^2\psi_{s,1}+\cos^2\zeta_{s,1})}, \quad (81)\end{aligned}$$

whereas, assuming a strong MUI ($\epsilon_1 \gg 1$), we obtain, for $M = 2$

$$\begin{aligned}\mathrm{SINR}_{R_{2,o}} &= \mathrm{SINR}_{R_{2,s}} = \mathrm{SINR}_{R_{2,sc}} \\ &\approx 2\epsilon_s(1-\cos^2\phi_{s,1}), \text{for } \phi_{s,1} \neq k\pi \quad (82)\\ &= \frac{2\epsilon_s}{1+2\epsilon_1}, \qquad \text{for } \phi_{s,1} = k\pi \quad (83)\\ \mathrm{SINR}_{QR_{2,o}} &= \mathrm{SINR}_{QR_{2,sc}} \approx 2\epsilon_s\,(1- \\ &\frac{(1+2\epsilon_s)(\cos^2\zeta_{s,1}+\cos^2\psi_{s,1})-4\epsilon_s\cos^2\zeta_{s,1}\cos^2\psi_{s,1}}{2[1+2\epsilon_s-\epsilon_s(\cos^2\zeta_{s,1}+\cos^2\psi_{s,1})]}\Big), \\ &\qquad \text{for } (\psi_{s,1},\zeta_{s,1}) \neq (k_1\pi,k_2\pi), \quad (84)\\ &\approx \frac{\epsilon_s}{\epsilon_1}, \text{ for } (\psi_{s,1},\zeta_{s,1}) = (k_1\pi,k_2\pi), \quad (85)\end{aligned}$$

Note that (84) reduces to (82) for synchronous SOI and MUI ($\tau_1 = 0$).

$$\mathrm{SINR}_{QR_{2,s}} \approx 2\epsilon_s\left(1-\frac{1+\cos^2\psi_{s,1}+2\epsilon_s(1-\cos^2\psi_{s,1})}{2[1+\epsilon_s(1-\cos^2\psi_{s,1})]}\right) =$$
$$\frac{\epsilon_s\sin^2\psi_{s,1}}{1+\epsilon_s\sin^2\psi_{s,1}}, \text{ for } \psi_{s,1} \neq k\pi \quad (86)$$
$$\approx \frac{9\epsilon_s}{2\epsilon_1(1+4\cos^2\zeta_{s,1})}, \text{ for } \psi_{s,1} = k\pi. \quad (87)$$

Furthermore, assuming $\epsilon_1 \gg 1$, we obtain, after cumbersome derivations, for $M = 3$

$$\begin{aligned}\mathrm{SINR}_{R_{3,s}} &\approx 2\epsilon_s(1-\cos^2\phi_{s,1}); \quad \phi_{s,1} \neq k\pi \quad (88)\\ &= \frac{2\epsilon_s}{1+2\epsilon_1}; \qquad \phi_{s,1} = k\pi \quad (89)\end{aligned}$$

whereas (78) reduces to

$$\begin{aligned}\mathrm{SINR}_{QR_{3,s}} &\approx 2\epsilon_s\left(1-\frac{\cos^2\psi_{s,1}+\cos^2\zeta_{s,1}}{2}\right); \\ &(\psi_{s,1},\zeta_{s,1}) \neq (k_1\pi,k_2\pi) \text{ and } \epsilon_s \ll 1 \quad (90)\\ &= \frac{2\epsilon_s}{1+2\epsilon_1}; (\psi_{s,1},\zeta_{s,1}) = (k_1\pi,k_2\pi). \quad (91)\end{aligned}$$

Again, for synchronous SOI and MUI, $\psi_{s,1} = \zeta_{s,1} = \phi_{s,1}$ and we verify that (90) corresponds to (88). Note that expressions (79) and (90), obtained for $\epsilon_s \ll 1$, correspond

to the SINR at the output of the three-input pseudo-MLSE receiver obtained in [33, (63) and (64)] for QR signals, which does not take into account the ISI in $z_{3_s}(k)$, which is processed by the Viterbi algorithm. Comparing (88) to (82), we deduce, for $\epsilon_1 \gg 1$, the following result:

$$\begin{aligned} \mathrm{SINR}_{R_{3,s}} &= \mathrm{SINR}_{R_{2,o}} = \mathrm{SINR}_{R_{2,s}} = \mathrm{SINR}_{R_{2,sc}} \\ &\approx 2\epsilon_s(1-\cos^2\phi_{s,1}); \quad \phi_{s,1} \neq k\pi, \end{aligned} \tag{92}$$

while comparing (90) to (84) and (86), we deduce, for $\epsilon_s \ll 1 \ll \epsilon_1$, that

$$\begin{aligned} \mathrm{SINR}_{QR_{3,s}} &= \mathrm{SINR}_{QR_{2,o}} = \mathrm{SINR}_{QR_{2,sc}} \\ \approx 2\epsilon_s &\left(1-\frac{\cos^2\psi_{s,1}+\cos^2\zeta_{s,1}}{2}\right); (\psi_{s,1},\zeta_{s,1}) \neq (k_1\pi, k_2\pi) \end{aligned} \tag{93}$$

$$\mathrm{SINR}_{QR_{2,s}} \approx 2\epsilon_s\left(1-\frac{1+\cos^2\psi_{s,1}}{2}\right). \tag{94}$$

c) *Analysis*

Let us recall that a receiver performs MAIC (for $N > 1$) or SAIC (for $N = 1$) as $\epsilon_1 \to \infty$, if the associated SINR does not converge toward zero. We deduce from (73), (80) and (81) that, for both R and QR signals, the conventional receivers ($M = 1$) perform MAIC as soon as $|\alpha_{s,1}| \neq 1$, but perform SAIC very scarcely, only when $\phi_{s,1} = (2k+1)\pi/2$ for R signals and when $(\tau_1/T, \phi_{s,1}) = (2k_1, (2k_2+1)\pi/2)$ or $(2k_1+1, k_2\pi)$ for QR signals, where k, k_1 and k_2 are integers.

Moreover, we deduce from (74) to (76) and (82) to (87) that, for both R and QR signals, the sc, o and s two-input MMSE receivers perform MAIC as soon as $|\alpha_{s,1}| \neq 1$, but perform SAIC as long as $\phi_{s,1} \neq k\pi$ for R signals, $(\psi_{s,1}, \zeta_{s,1}) \neq (k_1\pi, k_2\pi)$ for QR signals and receivers o and sc and $\psi_{s,1} \neq k\pi$ for QR signals and receiver s, enlightening the great interest of the three two-input MMSE receivers in both cases.

Moreover, we deduce from equations (73), (74), (80), (82) and (83) that for R signals, for both $M = 1$ and $M = 2$, the three o, s, sc M-input MMSE receivers are equivalent, discarding in this case the need to estimate the channel of the MUI and proving that the structure constraint has no impact on performance. Expression (73) shows that the equivalence of the three receivers also holds for QR signal for $M = 1$ as long as there is a spatial discrimination between the SOI and the MUI. However, despite similar processing and similar extended models (8) and (10) for R and QR signals respectively, the output SINRs (74) and (75), (76), for $|\alpha_{s,1}| \neq 1$, and (82), (84), (86) and (83), (85), (87) for $|\alpha_{s,1}| = 1$, correspond to different expressions. This proves the general non equivalence of R and derotated QR signals for the sc, o and s two-input MMSE receivers in the presence of MUI, result which has already been obtained for the two-input pseudo-ML receivers [33]. In particular, for a zero roll-off, while (74), only depends on $2\epsilon_s$, the maximum output SINR obtained without interference, and the parameters $\alpha_{s,1}$ and $\phi_{s,1}$, (75) and (76) depends not only on the previous parameters but also on τ_1/T. Note that the only equivalence between R and QR signals for two-input receivers is obtained for synchronous SOI and MUI for the o and sc receivers. Moreover, (75), (76) and (84) to (87) show that for QR signals and a zero roll-off, the s two-input MMSE receiver becomes sub-optimal with respect to o and sc two-input MMSE receivers, which are both equivalent in this case.

Finally, the previous results show, for SRRC filter with zero roll-off, a strong MUI (for R signals) and a strong MUI and a weak SOI (for QR signals), the optimality of the s three-input MMSE receiver. However, while it does not improve the performance of the s two-input MMSE receiver for R signals, since the latter is optimal, it outperforms the performance of the latter for QR signals since $\mathrm{SINR}_{QR_{3,s}} \geq \mathrm{SINR}_{QR_{2,s}}$.

d) Illustrations

To illustrate the previous results, Fig. 8a and 8b show, for the o, s two-input and the s three-input MMSE receivers, the variations of the output SINR as a function of $\phi_{s,1}$ for $\epsilon_s = 10$ dB, $\epsilon_1 = 20$ dB, synchronous ($\tau_1 = 0$) SOI and MUI and $|\phi_{s,1}| = 1$ ($N = 1$) (a), $|\phi_{s,1}| = 0.75$ (b). Similarly, in the same scenario, Fig. 9a and 9b show the variations of the output SINR as a function of τ_1 for $\phi_{s,1} = \pi/3$. Fig. 8a and 8b show, for synchronous SOI and MUI, for both R and QR signals and for the MMSE three receivers, an increasing output SINR as $\cos^2\phi_{s,1}$ decreases. Moreover, $\mathrm{SINR}_{QR_{2,s}}$ is lower for $\epsilon_s = 10$ dB than for $\epsilon_s \ll 1$, due to ISI. Finally, note for $N = 1$, the equivalent optimal performance of the three receivers, except the s two-input receiver for QR signals which is clearly sub-optimal. Note for $N > 1$, the equivalent quasi-optimal performance of the s three-input receiver for R and QR signals and the sub-optimal performance of the s two-input receiver for QR signals. Fig. 9 clearly shows, for R signals, optimal performance, independent of τ_1, for the three receivers contrary to QR signals for which output performance depend on τ_1. Note, in this case, quasi-optimal performance of the s three-input receiver and sub-optimal performance of the s two-input receiver. Note finally, for $\tau_1 \neq 2kT$ (with k integer), lower performance of the optimal receiver for QR signals with respect to R ones, showing again the non equivalence of R and QR signals for optimal two-input MMSE receivers.

C3) *Deterministic channels and SRRC filters (for T) with arbitrary roll-off:* To compare, for R and QR signals, the performance of the sc, o, M-input ($M = 1, 2$) and the s M-input ($M = 1, 2, 3$) MMSE receivers, for $\omega = 0$ and arbitrary values of τ_1 and also to extend the analysis to arbitrary values of the roll-off ω, we must adopt a statistical perspective. For this purpose, we still consider deterministic channels, we assume that $(\phi_{s,1}, \tau_1)$ are independent random variables uniformly distributed on $[0, 2\pi] \times [0, 4T]$ and we

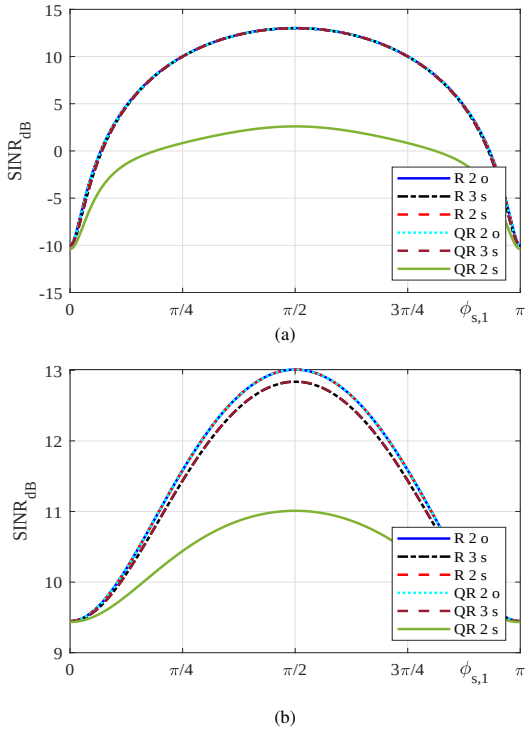

Fig. 8. SINR_R and SINR_{QR} as a function of $\phi_{s,1}$ ($|\alpha_{s,1}| = 1$ (a), $|\alpha_{s,1}| = 0.75$ (b), $\epsilon_s = 10$ dB, $\epsilon_1 = 20$ dB, $\tau_1 = 0$, $\omega = 0$ deterministic channels.

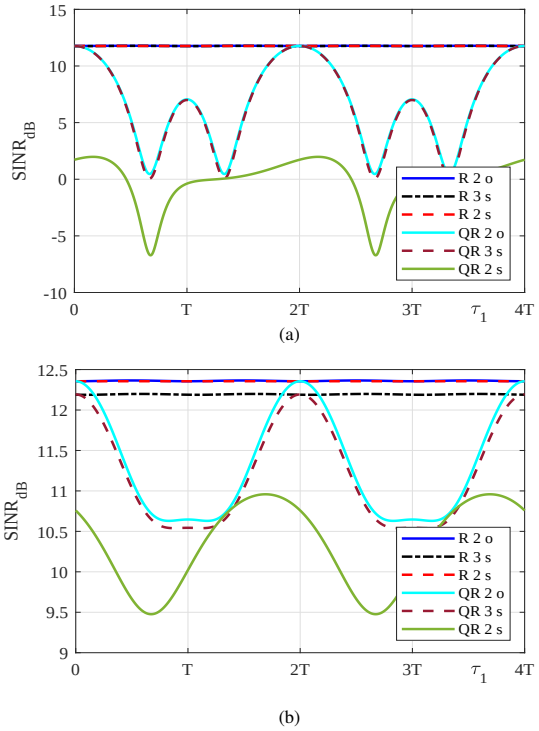

Fig. 9. SINR_R and SINR_{QR} as a function of τ_1 ($|\alpha_{s,1}| = 1$ (a), $|\alpha_{s,1}| = 0.75$ (b), $\epsilon_s = 10$ dB, $\epsilon_1 = 20$ dB, $\phi_{s,1} = \pi/3$, $\omega = 0$ deterministic channels.

choose $\epsilon_s = 10$ dB and $\epsilon_1 = 20$ dB.

Under these assumptions, Figs 10 and 11 show, for R and QR signals respectively, for $N = 1$, $\omega = 0$, the variations of $\Pr[(\mathrm{SINR}_{M_g}/2\epsilon_s)\mathrm{dB} \geq x\mathrm{dB}] \stackrel{\mathrm{def}}{=} P_{M_g}(x)$ as a function of x (dB) for the sc, o and s M-input MMSE receivers for $M = 1, 2$. Figs. 12 and 13 show the same variations as 10 and 11, but for $\omega = 1$. Finally, Figs. 14 and 15 show, for $\omega = 0$ (Fig. 14a and Fig. 15a) and $\omega = 1$ (Fig. 14b and Fig. 15b), the same variations as Figs 10 and 11 but for the sc and o two-input and the s two-input and three-input MMSE receivers. Note that the curves appearing in these figures are built from 10^5 Monte-Carlo simulations. Note, for both R and QR signals, poor performance whatever ω of the one-input MMSE receivers, i.e., of the conventional receivers.

Note for R signals, quasi-optimal performance of the sc and s two-input MMSE receivers for low values of ω and a slight increasing sub-optimality of these receivers as ω increases. Note increasing performance with the roll-off of the s three-input MMSE receiver, which is quasi-optimal whatever the roll-off and which always improves the performance of the s two-input MMSE receiver. This proves, for channels with no delay spread and arbitrary values of ω, the great interest of sc two-input, s two-input and s-three input MMSE receivers for R signals.

Note for QR signals, quasi-optimal performance of the

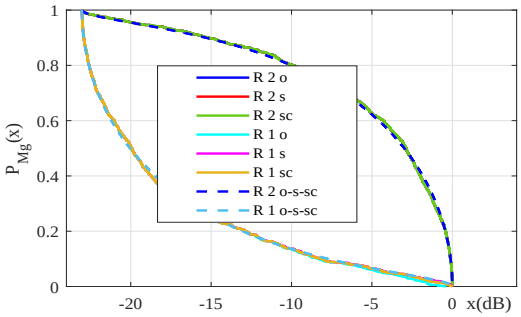

Fig. 10. $\mathrm{P}_{M_g}(x)$ as a function of x ($N = 1$, $M = 1, 2$, ϵ_s = 10 dB, ϵ_1 = 20 dB, $\omega = 0$, deterministic channels, R signals.

sc two-input MMSE receiver for low values of ω, a slight increasing sub-optimality of this receiver as ω increases and a sub-optimality of s two-input MMSE receiver whatever the roll-off. This proves also the necessity to improve the s two-input MMSE receiver for QR signals. Note the quasi-optimal performance, whatever the roll-off value, and then the practical interest of the s three-input MMSE receiver, strongly improving the performance of the s two-input receiver.

C4) *Deterministic channels and MSK and GMSK signals:* Figs. 16 and 17 show the same variations as Fig. 15 under the same assumptions, but for MSK and GMSK QR

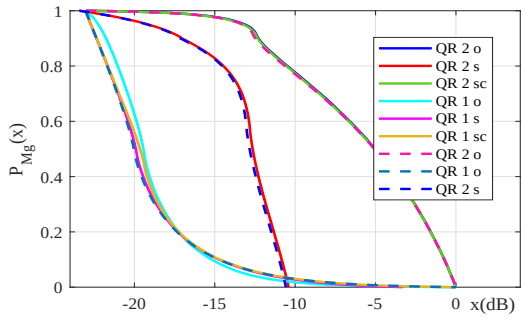

Fig. 11. $P_{M_g}(x)$ as a function of x ($N = 1$, $M = 1, 2$, ϵ_s = 10 dB, ϵ_1 = 20 dB, $\omega = 0$, deterministic channels, $\pi/2$-ASK QR signals.

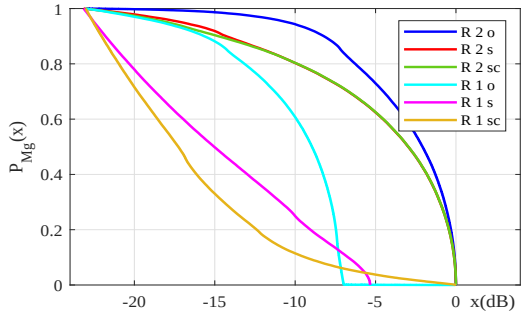

Fig. 12. $P_{M_g}(x)$ as a function of x ($N = 1$, $M = 1, 2$, ϵ_s = 10 dB, ϵ_1 = 20 dB, $\omega = 1$, deterministic channels, R signals.

signals respectively. We still note, in both cases, the worst performance of the s two-input MMSE receiver, the sub-optimality of the sc two-input MMSE receiver and the quasi-optimal performance of the s three-input MMSE receiver, strongly improving the performance of the s two-input MMSE receiver. We also note better performance obtained for the MSK signals with respect to GMSK signals due to a greater power on the cyclic frequency $\beta_{d,-1} = -1/T$ [35], [40].

C5) *Rayleigh channels and SRRC filters (for T) with arbitrary roll-off:* To complete the previous results, we consider the assumptions of Figs. 14b and 15b for R and QR signals respectively. Under these assumptions, Fig. 18 shows, for R and QR signals and for $\omega = 1$ the same variations as Figs. 14b and 15b but for Rayleigh fading channels for which $h(1)$ and $h_1(1)$ are i.i.d zero mean circular Gaussian distributed random variables. The conclusions of Figs. 14b and 15b hold for Figs. 18a and 18b with less sub-optimality of s and sc two-input MMSE receivers with respect to s three-input and o two-input MMSE receivers.

F. SINR analysis for one MUI and two tap deterministic channel

We consider in this sub-section a one-tap deterministic channel for the SOI and a two-tap frequency selective

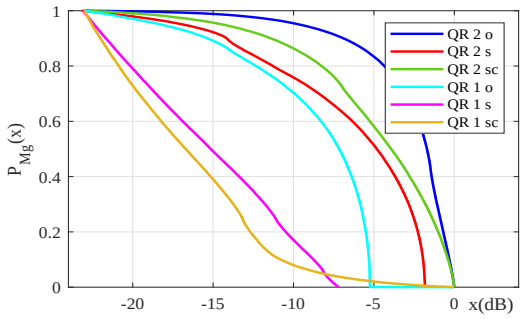

Fig. 13. $P_{M_g}(x)$ as a function of x ($N = 1$, $M = 1, 2$, ϵ_s = 10 dB, ϵ_1 = 20 dB, $\omega = 1$, deterministic channels, $\pi/2$-ASK QR signals.

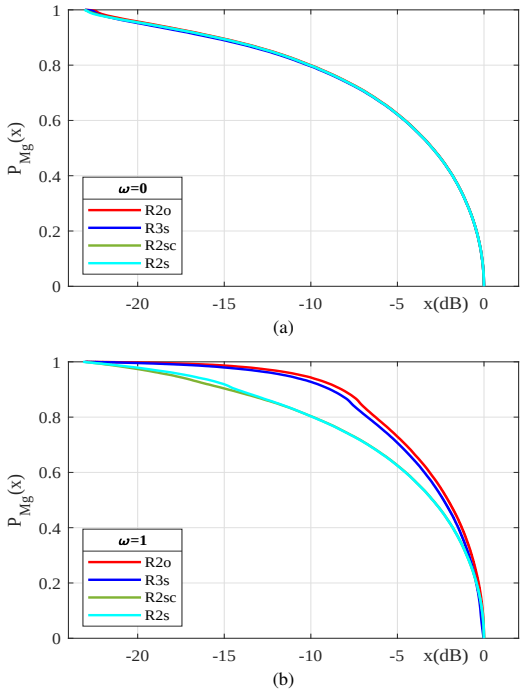

Fig. 14. $P_{M_g}(x)$ as a function of x ($N = 1$, $M = 2, 3$, ϵ_s = 10 dB, ϵ_1 = 20 dB, $\omega = 0$ (a) and 1 (b), deterministic channel, R signals.

deterministic channel for the MUI such that

$$\begin{aligned} \mathbf{h}(t) &= \mu\delta(t)\mathbf{h} \\ \mathbf{h}_1(t) &= \mu_{1_1}\delta(t-\tau_1)\mathbf{h}_{1_1} + \mu_{1_2}\delta(t-\tau_1-T)\mathbf{h}_{1_2}, \end{aligned} \quad (95)$$

where μ_{1_1} and μ_{1_2} control the amplitudes of the first and second paths of the MUI, whereas $\mathbf{h}_{1_1}$ and $\mathbf{h}_{1_2}$ correspond to the channel vectors of the latter, such that $\|\mathbf{h}_{1_1}\|^2 = \|\mathbf{h}_{1_2}\|^2 = N$. Under these assumptions and for SRRC pulse shaping filters for T, it is straightforward to verify that $\pi_1 = (\mu_{1_1}^2 + \mu_{1_2}^2)\pi_{b_1}$. We assume that $(\phi_{s,1_1}, \phi_{s,1_2}, \tau_1)$ are r.v. uniformly distributed on $[0, 2\pi] \times [0, 2\pi] \times [0, 4T]$, where $\phi_{s,1_1}$ and $\phi_{s,1_2}$ are the phases of $\mathbf{h}^H\mathbf{h}_{1_1}$ and $\mathbf{h}^H\mathbf{h}_{1_2}$, respectively. Under these assumptions, Figs. 19a and 19b

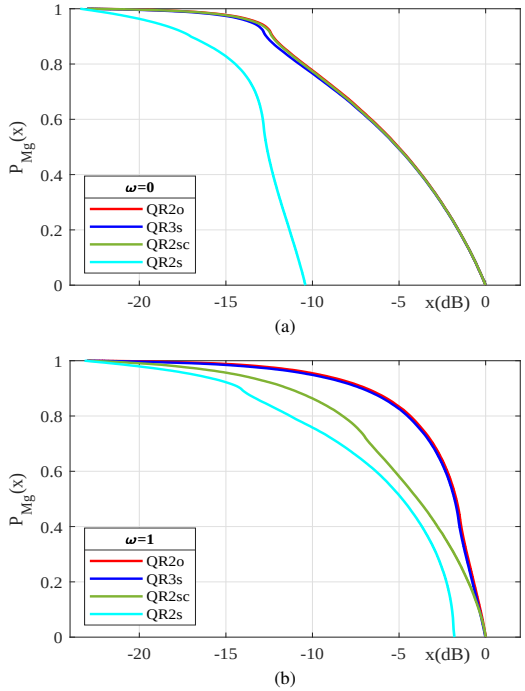

Fig. 15. $P_{M_g}(x)$ as a function of x ($N = 1$, $M = 2, 3$, ϵ_s = 10 dB, ϵ_1 = 20 dB, $\omega = 0$ (a) and 1 (b), deterministic channel, $\pi/2$-ASK QR signals.

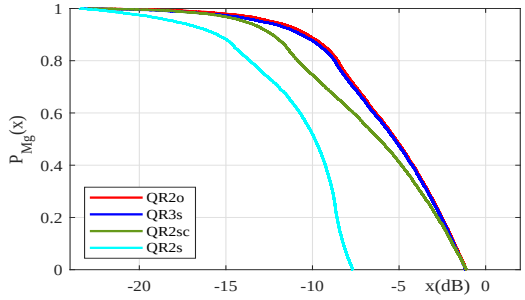

Fig. 16. $P_{M_g}(x)$ as a function of x ($N = 1$, $M = 2, 3$, ϵ_s = 10 dB, ϵ_1 = 20 dB, deterministic channel, MSK signals.

show, for R and QR signals, respectively and for $\omega = 1$, the same variations as Figs. 14b and 15b for $\mu_{1_1} = \mu_{1_2}$. The conclusions of Figs. 14b and 15b hold for Figs. 19a and 19b.

V. SER at the output of the M-input MMSE receivers for one MUI

We show in this section that the main messages of the previous section, deduced from an output SINR analysis remain valid from an output SER analysis.

A. Theoretical closed-form expressions

To compare the previous M-input MMSE receivers ($M = 2, 3$) for R and QR signals from an output SER analysis,

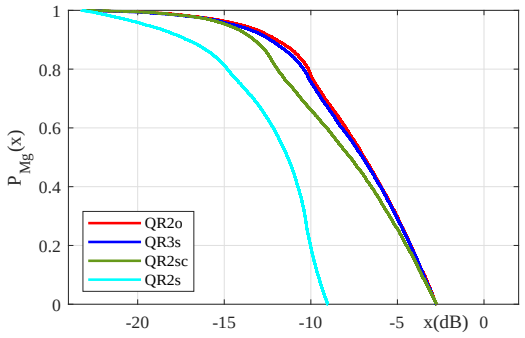

Fig. 17. $P_{M_g}(x)$ as a function of x ($N = 1$, $M = 2, 3$, ϵ_s = 10 dB, ϵ_1 = 20 dB, deterministic channel, GMSK signals.

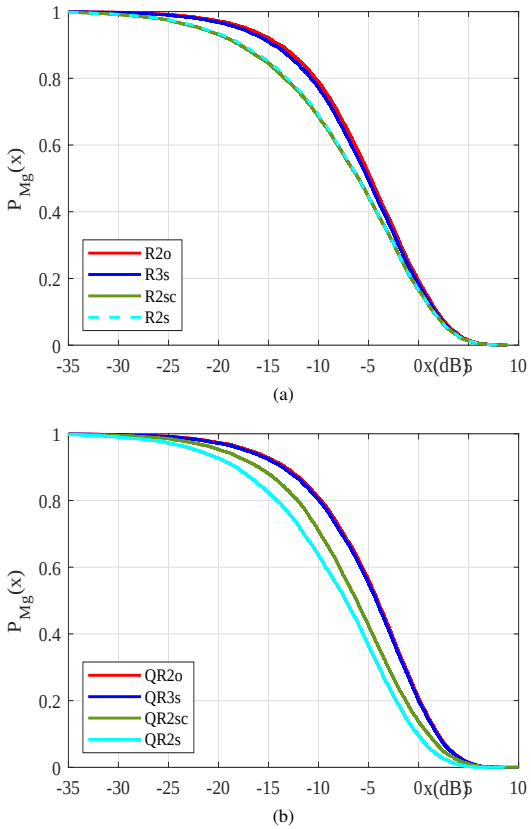

Fig. 18. $P_{M_g}(x)$ as a function of x ($N = 1$, $M = 2, 3$, ϵ_s = 10 dB, ϵ_1 = 20 dB, $\omega = 1$, Rayleigh channel, (a) R and (b) $\pi/2$-ASK QR signals.

we still assume in this section that the total noise $\mathbf{n}(t)$ is composed of a Gaussian distributed background noise $\boldsymbol{\epsilon}(t)$ and a single MUI, which generates the observation model (13) with $P = 1$. From (13), we get the generic real part, $z_{M_g}(k)$, of the generic output $y_{M_g}(k)$, of the different M-

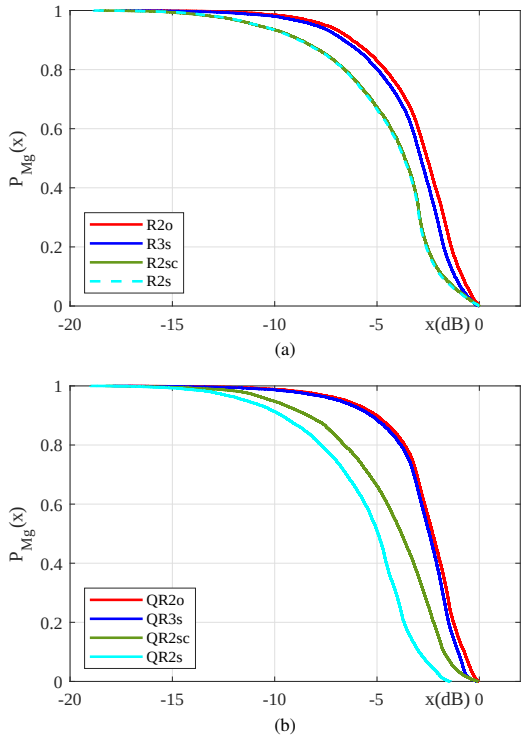

Fig. 19. $\mathrm{P}_{M_g}(x)$ as a function of x ($N = 1$, $M = 2, 3$, ϵ_s = 10 dB, ϵ_1 = 20 dB, $\mu_{1_1} = \mu_{1_2}$, $\omega = 1$, deterministic two-taps channel, (a) R and (b) $\pi/2$-ASK QR signals.

input MMSE receiver for $g = o, s, sc$.

$$z_{M_g}(k) = \underbrace{b_k u_{M_{g,0}}}_{\text{SOI}} + \underbrace{\sum_{\ell \neq k} b_\ell u_{M_{g,k-\ell}}}_{\text{ISI}} + \underbrace{\sum_{\ell} b_{1,\ell} u_{M_{1,g,k-\ell}}}_{\text{MUI}} + \underbrace{\epsilon_{M_g}(k)}_{\text{BN}} \quad (96)$$

where $u_{M_{g,k}} \overset{\text{def}}{=} \mathrm{Re}[\int \mathbf{w}_{M_g}^H(f)\mathbf{g}_{M_g}(f)e^{j2\pi fkT}df]$, $u_{M_{1,g,,k}} \overset{\text{def}}{=} \mathrm{Re}[\int \mathbf{w}_{M_g}^H(f)\mathbf{g}_{1,M_g}(f)e^{j2\pi fkT}df]$ and $\epsilon_{M_g}(k) \overset{\text{def}}{=} \mathrm{Re}[\int \mathbf{w}_{M_g}^H(f)\boldsymbol{\epsilon}_{M_g}(f)e^{j2\pi fkT}df]$ is the background noise (BN) component which is zero-mean Gaussian distributed with variance $\sigma^2_{\epsilon_{M_g}}$ whose expression is derived in Appendix E.

When the number of ISI and MUI terms at the output of the M-input MMSE receivers is large and when there are no dominant term in the ISI and MUI, an approximation of the central limit theorem (Lyapounov theorem [41, th. 27.3]) for independent non identically distributed r.v. can be applied and the SER is directly deduced from the SINR. For example, for BPSK symbols b_k and $b_{1,k}$, we get the approximation:

$$\mathrm{SER}_{M_g} \approx Q(\sqrt{\mathrm{SINR}_{M_g}}), \quad (97)$$

with $Q(x) \overset{\text{def}}{=} \int_x^{+\infty} \frac{1}{\sqrt{2\pi}} e^{-\frac{u^2}{2}} du$. This relation (97) confirms that the performance in term of output SINR and SER are equivalent.

When this number of ISI and MUI terms is weak and/or there is a dominant term in the ISI or MUI, the approximation is no longer valid, but an exact analytical expression of the SER can be derived. If $\mathcal{S}$ and $\mathcal{I}$ denote the sets of the ISI and MUI symbols, respectively, with respect to the symbol b_0, we now get by conditioning with respect to these BPSK symbols where $\mathcal{S} = \{-1, +1\}^{|\mathcal{S}|}$ and $\mathcal{I} = \{-1, +1\}^{|\mathcal{I}|}$:

$$\mathrm{SER}_{M_g} = \frac{1}{2^{|\mathcal{S}|}2^{|\mathcal{I}|}} \sum_{(..,b_{-1},b_{+1},..)\in\mathcal{S}} \sum_{(..,b_{1,-1},b_{1,0},b_{1,+1},..)\in\mathcal{I}} Q\left(\frac{u_{M_{g,0}} - (\sum_{k\neq 0} b_k u_{M_{g,k}} + \sum_k b_{1,k} u_{M_{1,g,k}})}{\sigma_{\epsilon_{M_g}}}\right). \quad (98)$$

B. Monte-Carlo experiments

When the conditions for which (97) can apply are not satisfied, we can resort to (98) for BPSK modulations. But this closed-form expression presents no engineering insights and shows that the SER and SINR are not directly related. To confirm that the results obtained in Section IV for output SINR are still vaild for output SER, we present in the following some Monte Carlo simulations.

B1) *One tap deterministic channels:* We consider the transmission of 1000 frames of 200 binary symbols ($b_k \in \{-1, +1\}$ and $b_{1,k} \in \{-1, +1\}$) and we assume, in this subsection, one tap deterministic channels which are constant over a frame and random from a frame to another. For each frame, we assume that $(\phi_{s,1}, \tau_1)$ are i.i.d. uniformly distributed on $[0, 2\pi] \times [0, 4T]$. Under these assumptions, Fig. 20 shows the variations of the SER given by the binary detector at the output of the different receivers for both R (BPSK) and QR ($\pi/2$-BPSK) signals, as a function of ϵ_s for $N = 1$, $\epsilon_1/\epsilon_s = 10$ dB and $\omega = 1$.

The results of Fig. 20 confirm, for both R and QR signals and from a SER perspective, the sub-optimality of the s and sc two-input receivers and the quasi-optimality of the s three-input MMSE receiver.

B2) *One tap Rayleigh channels:* To complete the previous results and under the assumptions of Fig. 20, Fig. 21 shows the same variations as Fig. 20, but as a function of $\mathrm{E}(\epsilon_s)$ for Rayleigh fading channels for which $h(1)$ and $h_1(1)$ are zero-mean circular Gaussian independently distributed, such that $\mathrm{E}[\epsilon_1]/\mathrm{E}[\epsilon_s] = 10$ dB. The conclusions of Fig. 20 hold for Fig. 21.

VI. Conclusion

New insights into linear but especially WL MMSE receivers have been given in this paper, for both R and QR signals, omnipresent in numerous present and future applications, in the absence but mainly in the presence of data-like MUI, for propagation channels with or without

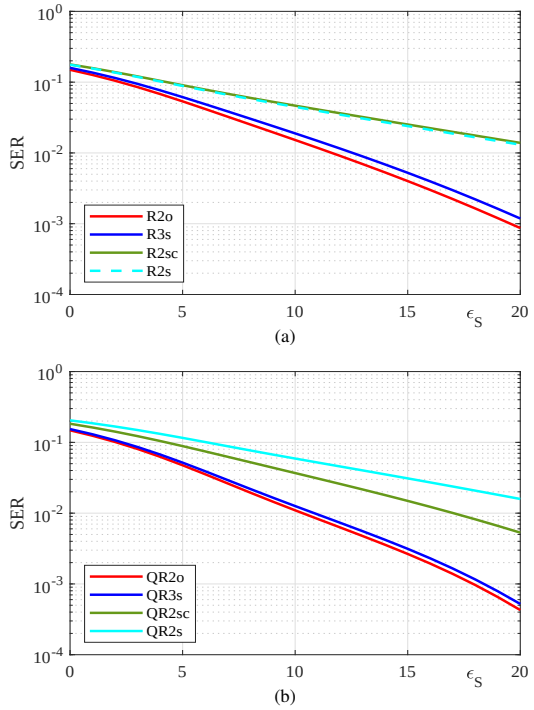

Fig. 20. SER as a function of ϵ_s ($N = 1$, $\epsilon_1/\epsilon_s = 10$ dB, $\omega = 1$, deterministic one tap channel, R (a) and $\pi/2$-ASK QR (b) signals.

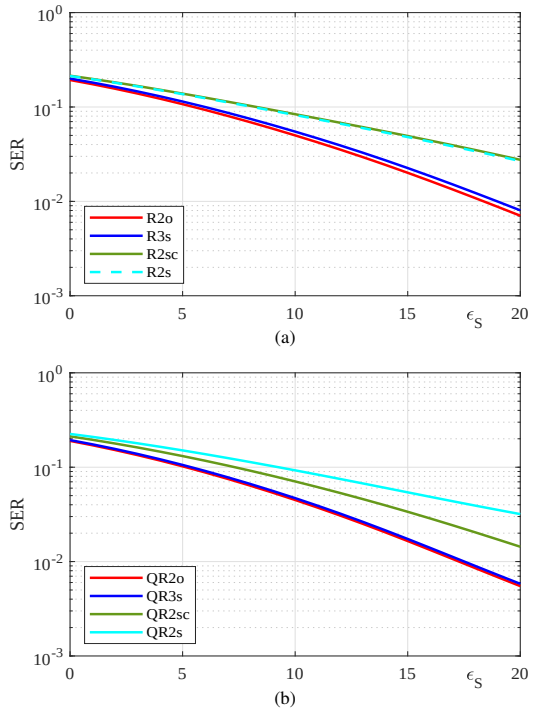

Fig. 21. SER as a function of $\mathrm{E}(\epsilon_s)$ ($N = 1$, $\mathrm{E}(\epsilon_1)/\mathrm{E}(\epsilon_s) = 10$ dB, $\omega = 1$, Rayleigh fading one tap channel, R and $\pi/2$-ASK QR signals.

delay spread and using a CT approach. Several R signals, such as BPSK and ASK signals, and QR signals, such as $\pi/2$-BPSK, $\pi/2$ASK, OQAM, MSK and GMSK signals, have been considered. It was first recalled that most of the WL MMSE receivers of the literature correspond to two-input MMSE receivers which are implemented at the symbol rate, after a matched filtering operation to the pulse shaping filter and have thus a particular structure constraint. It has been shown in this paper that most of these receivers are equivalent to each other and correspond to the sc two-input MMSE receiver, which does not require the knowledge of the MUI channels, contrary to what is generally implicitly assumed in the literature. However, this receiver has been shown, to be generally sub-optimal in frequency selective channels and in the presence of MUI. The optimal WL or two-input MMSE receiver, denoted by o two-input MMSE receiver, has been computed. It has no structure constraint, exploits the MUI waveform or their cyclostationarity but requires the knowledge or estimation of the MUI channels, which may be cumbersome in practice. The main challenge addressed in this paper was then to develop new WL MMSE receivers able to implement the optimal one without requiring the knowledge of the MUI channels. To this aim, a first new WL MMSE receiver, falsely assuming SO stationary MUI and denoted by s two-input MMSE receiver, has been proposed. It only requires the knowledge or the estimation of the SOI channel, hence its practical interest. Its performance, in terms of output SINR on the current symbol before decision and in terms of output SER, have been computed both analytically and by computer simulations and compared to those of the o two-input MMSE receiver. For R signals and SRRC filters, the s two-input MMSE receiver has been shown to be quasi-optimal for low values of the roll-off, whereas its sub-optimality increases as the roll-off increases. For QR signals, the s two-input MMSE receiver has been shown to be always sub-optimal whatever the value of the roll-off, showing in particular the non equivalence of R and QR signals for MMSE processing, due to different SO cyclostationarity properties. For this reason a second new WL MMSE receiver corresponding to a three-input FRESH MMSE receiver, still falsely assuming SO stationary MUI and denoted by s three-input MMSE receiver, has been proposed. It still only requires the knowledge or the estimation of the SOI channel, hence its practical interest. The performance analysis of this new receiver has shown the quasi-optimality of this three-input MMSE receiver for both R and QR signals, and whatever the value of the roll-off. This result has been extended to MSK and GMSK signals. This interesting result open new perspectives for the implementation optimization of WL MMSE receivers in the presence of R and QR data-like MUI and, in particular, for the implementation of the o WL MMSE receiver from the only knowledge of the SOI channel.

APPENDIX

A. Proofs related to the sc M-input MMSE receivers

1) Proof of (17)*:* Because the samples $\mathbf{x}_{v,M}(kT)$ of $\mathbf{x}_{v,M}(t)$ given by (15) are SO stationary, $y_{M_{sc}}(k)$, defined by (22), is also SO stationary. From (39), where b_k and $e_{M_{sc}}(k)$ are uncorrelated, and from $u_{M_{sc}} = T\int_\Delta \mathbf{w}_{M_{sc}}^{d^H}(f)\mathbf{g}_{v,M}^d(f)df$, the MSE = $\mathrm{E}(|b_k - y_{M_{sc}}(k)|^2)$ is given by:

$$\begin{aligned}
&\mathrm{MSE}\\
&= \pi_b|1-u_{M_{sc}}|^2 + \mathrm{E}|e_{M_{sc}}(k)|^2 \qquad (99)\\
&= \pi_b|1-u_{M_{sc}}|^2 + \mathrm{E}|y_{M_{sc}}(k)|^2 - \pi_b|u_{M_{sc}}|^2\\
&= \mathrm{E}|y_{M_{sc}}(k)|^2 + \pi_b(1-u_{M_{sc}}-u_{M_{sc}}^*)\\
&= T\int_\Delta \Big[\mathbf{w}_{M_{sc}}^{d^H}(f)\mathbf{R}_{x_{v_M}}^d(f)\mathbf{w}_{M_{sc}}^d(f)\\
&+ \pi_b\left(1-\mathbf{w}_{M_{sc}}^{d^H}(f)\mathbf{g}_{v_M}^d(f)-\mathbf{w}_{M_{sc}}^{d^T}(f)\mathbf{g}_{v_M}^{d*}(f)\right)\Big]df, \qquad (100)
\end{aligned}$$

whose function in the integral (100) is classically minimized by $\mathbf{w}_{M_{sc}}^d(f)$ given by (17) for the frequencies such that $\mathbf{x}_{v,M}^d(f) \neq 0$. ■

2) Proof of (23)*:* Similarly, the output $\mathbf{y}_{M_{sc}}(k)$ of the filter $\mathbf{W}_{M_{sc}}^{d^*}(f)$ is SO stationary and

$$\mathbf{y}_{M_{sc}}(k) = \mathbf{U}_{M_{sc}}\mathbf{b}_k + \mathbf{e}_{M_{sc}}(k), \qquad (101)$$

where $\mathbf{U}_{M_{sc}} \stackrel{\mathrm{def}}{=} \int_\Delta \mathbf{W}_{M_{sc}}^{d^H}(f)\mathbf{G}_{v_M}^d(f)df$ and where $\mathbf{b}_k$ and $\mathbf{e}_{M_{sc}}(k)$ are uncorrelated. This implies that the JMSE = $\mathrm{E}\|\mathbf{b}_k - \mathbf{y}_{M_{sc}}(k)\|^2$ is given by:

$$\begin{aligned}
&\mathrm{JMSE}\\
&= \mathrm{E}\|(\mathbf{U}_{M_{sc}}-\mathbf{I}_{P+1})\mathbf{b}_k\|^2 + \mathrm{E}\|\mathbf{e}_{M_{sc}}(k)\|^2\\
&= \mathrm{E}\|(\mathbf{U}_{M_{sc}}-\mathbf{I}_{P+1})\mathbf{b}_k\|^2 + \mathrm{E}\|\mathbf{y}_{M_{sc}}(k)\|^2 - \mathrm{E}\|\mathbf{U}_{M_{sc}}\mathbf{b}_k\|^2\\
&= \mathrm{E}\|\mathbf{y}_{M_{sc}}(k)\|^2 + \pi_b\mathrm{Tr}[(\mathbf{U}_{M_{sc}}-\mathbf{I}_{P+1})(\mathbf{U}_{M_{sc}}-\mathbf{I}_{P+1})^H]\\
&- \pi_b\mathrm{Tr}(\mathbf{U}_{M_{sc}}\mathbf{U}_{M_{sc}}^H)\\
&= T\int_\Delta \mathrm{Tr}[\mathbf{W}_{M_{sc}}^{d^H}(f)\mathbf{R}_{x_{v_M}}^d(f)\mathbf{W}_{M_{sc}}^d(f)\\
&+\pi_b(\mathbf{I}_{P+1}-\mathbf{W}_{M_{sc}}^{d^H}(f)\mathbf{G}_{v_M}^d(f)-\mathbf{W}_{M_{sc}}^{d^T}(f)\mathbf{G}_{v_M}^{d*}(f))]df \qquad (102)
\end{aligned}$$

and is minimized for

$$\mathbf{W}_{M_{sc}}^d(f) = \pi_b[\mathbf{R}_{x_{v_M}}^d(f)]^{-1}\mathbf{G}_{v_M}^d(f), \qquad (103)$$

whose first column is $\mathbf{w}_{M_{sc}}^d(f)$ (23). ■

3) Proof of (48) *and* (49)*:* It follows that the derived structured MMSE receiver $\mathbf{w}_{M_{sc}}^d(f)$ gives

$$u_{M_{sc}} = T\int_\Delta \mathbf{g}_{M_{sc}}^{d^H}(f)[\mathbf{R}_{x_{v_M}}^d(f)]^{-1}\mathbf{g}_{M_{sc}}^d(f)df \qquad (104)$$

that is real-valued and besides (22) gives:

$$\begin{aligned}
&\mathrm{E}(|y_{M_{sc}}(k)|^2)\\
&= T\int_\Delta \mathbf{w}_{M_{sc}}^{d^H}(f)\mathbf{R}_{x_{v_M}}^d(f)\mathbf{w}_{M_{sc}}^d(f)df\\
&= T\pi_b^2\int_\Delta \mathbf{g}_{M_{sc}}^{d^H}(f)[\mathbf{R}_{x_{v_M}}^d(f)]^{-1}\mathbf{g}_{M_{sc}}^d(f)df \qquad (105)\\
&\mathrm{E}(y_{M_{sc}}^2(k))\\
&= T\int_\Delta \mathbf{w}_{M_{sc}}^{d^H}(f)\mathbf{C}_{x_{v_M}}^d(f)\mathbf{w}_{M_{sc}}^{d^*}(-f)df \qquad (106)\\
&= T\pi_b^2\int_\Delta \mathbf{g}_{v_M}^{d^H}(f)[\mathbf{R}_{x_{v_M}}^d(f)]^{-1}\mathbf{C}_{x_{v_M}}^d(f)\\
&\qquad [\mathbf{R}_{x_{v_M}}^{d^*}(-f)]^{-1}\mathbf{g}_{v_M}^{d^*}(-f)df. \qquad (107)
\end{aligned}$$

Using (104), (105) and (107) in (41), (48) and (49) follow for $M = 1$ and $M = 2$, respectively. ■

B. Proofs related to the o M-input MMSE receivers

1) Proof of (25)*:* Once the SO cyclostationarity of MUI is fully exploited, estimating the SOI symbols only or jointly with the MUI symbols gives rise to two equivalent approaches for the SOI symbols estimation.

In the jointly estimation approach, we deduce from (13) that the filter $\mathbf{w}_M^*(-t)$ minimizing the MSE criterion corresponds to the first column of the matrix $\mathbf{W}_M^*(-t)$, of dimension $N \times (P+1)$ for $M = 1$ and $2N \times (P+1)$ for $M = 2$, minimizing the joint MSE criterion, JMSE = $\mathrm{E}(\|\mathbf{b}_n - \mathbf{y}_M(nT)\|^2)$. In the latter criterion, $\mathbf{b}_n \stackrel{\mathrm{def}}{=} [b_n, b_{1,n}, ..b_{P,n}]^T$, whereas $\mathbf{y}_M(t)$ is defined by (24) where $\mathbf{w}_M(-f)$ is replaced by matrix $\mathbf{W}_M(-f)$. Noting that the JMSE criterion satisfies $\mathrm{E}\|\mathbf{b}_k - \mathbf{y}_M(kT)\|^2 = \mathrm{E}|b_k - y_M(kT)|^2 + \sum_{p=1}^P \mathrm{E}|b_{p,k} - y_{M,p}(kT)|^2$ where $y_{M,p}(t) = \mathbf{w}_{M,p}^*(-t) \otimes \mathbf{x}_M(t)$ and $\mathbf{W}_M(f) = [\mathbf{w}_M(f), \mathbf{w}_{M,1}(f), .., \mathbf{w}_{M,p}(f), .., \mathbf{w}_{M,P}(f)]$, the optimal MMSE filter $\mathbf{w}_{M_o}(f)$ is the first column of the optimal joint MMSE filter $\mathbf{W}_{M_o}(f)$. The output, at time kT of the filter matrix $\mathbf{W}_M^*(f)$ corresponds to the SO stationary signal:

$$\mathbf{y}_M(k) = \mathbf{U}_M(0)\mathbf{b}_k + \sum_{\ell\neq k}\mathbf{U}_M(k-\ell)\mathbf{b}_\ell + \boldsymbol{\epsilon}_{w,M}(k), \qquad (108)$$

where $\mathbf{U}_M(\ell) \stackrel{\mathrm{def}}{=} \int \mathbf{W}_M^H(f)\mathbf{G}_M(f)e^{j2\pi f\ell T}df$ and $\boldsymbol{\epsilon}_{w,M}(k) \stackrel{\mathrm{def}}{=} \int \mathbf{W}_M^H(f)\boldsymbol{\epsilon}_M(f)e^{j2\pi fkT}df$. Consequently the

JMSE criterion is given by:

$$\begin{aligned}\text{JMSE} &= \pi_b \text{Tr}[(\mathbf{U}_M(0)-\mathbf{I}_{P+1})(\mathbf{U}_M(0)-\mathbf{I}_{P+1})^H] \\ &+ \pi_b \sum_{\ell\neq 0} \text{Tr}[\mathbf{U}_M(\ell)\mathbf{U}_M^H(\ell)] \\ &+ \text{Tr}[\text{E}(\boldsymbol{\epsilon}_{w,M}(k)\boldsymbol{\epsilon}_{w,M}^H(k))] \\ &= \pi_b T \int_\Delta \text{Tr}[(\mathbf{I}_{P+1}-\sum_\ell \mathbf{U}_M(\ell)e^{-j2\pi\ell fT}) \\ &\qquad (\mathbf{I}_{P+1}-\sum_\ell \mathbf{U}_M(\ell)^{-j2\pi\ell fT})^H]df \\ &+ \text{Tr}[\text{E}(\boldsymbol{\epsilon}_{w,M}(k)\boldsymbol{\epsilon}_{w,M}^H(k))] \\ &= \pi_b T \int_\Delta \text{Tr}\big[\big(\mathbf{I}_{P+1}-\frac{1}{T}\sum_\ell \mathbf{W}_M^H(f-\frac{\ell}{T}) \\ &\mathbf{G}_M(f-\frac{\ell}{T})\big)\big(\mathbf{I}_{P+1}-\frac{1}{T}\sum_\ell \mathbf{W}_M^H(f-\frac{\ell}{T})\mathbf{G}_M(f-\frac{\ell}{T})\big)^H\big]df \\ &+ N_0 \int_\Delta \text{Tr}\big[\sum_\ell \mathbf{W}_M^H(f-\frac{\ell}{T})\mathbf{W}_M(f-\frac{\ell}{T})\big]df, \end{aligned} \quad (109)$$

where we have used the property $T\int_\Delta e^{-j2\pi\ell fT}df = \delta(0)$ in the fourth line. This JMSE is a quadratic functional of $\mathbf{W}_M(f-\frac{k}{T})$, $k\in\mathbb{Z}$. Following a standard method of the calculus of variations (see e.g., [42]), the JMSE (109) is minimized by $\mathbf{W}_{M_o}(f)=\mathbf{G}_M(f)\mathbf{C}_M^d(f)$ where $\mathbf{C}_M^d(f)=\big[(N_0/\pi_b)\mathbf{I}_{P+1}+1/T\sum_\ell \mathbf{G}_M^H(f-\ell/T)\mathbf{G}_M(f-\ell/T)\big]^{-1}$. ■

Whereas this jointly estimation approach involves that the additive noise is SO stationary, considering the estimation of the SOI symbols only involves that the total noise is SO cyclostationary, which implies a more complicated derivation derived in the following. We consider here the MSE $\text{E}|b_k-y_M(kT)|^2$ with $y_M(t)=\mathbf{w}_M^*(-t)\otimes\mathbf{x}_M(t)$ where the SO cyclostationarity of the MUI is taken into account. In this case, the CT total noise output $n_{M,w}(t)=\mathbf{w}_M^*(-t)\otimes\mathbf{n}_M(t)$ is SO cyclostationary with cyclic frequencies $\gamma_i=\alpha_i=i/T$ with power at times kT

$$\text{E}[|n_{M,w}^2(k)|] = \sum_{\gamma_i} e^{j2\pi\gamma_i kT}\int r_{n_{M,w}}^{\gamma_i}df \quad (110)$$

with

$$r_{n_{M,w}}^{\gamma_i}(f) = \mathbf{w}_M^H(f+\gamma_i/2)\mathbf{R}_{n_M}^{\gamma_i}(f)\mathbf{w}_M(f-\gamma_i/2) \quad (111)$$

where

$$\begin{aligned}\mathbf{R}_{n_M}^{\alpha_i}(f) &= \sum_{1\leq p\leq P}\frac{\pi_b}{T}[\mathbf{g}_{p,M}(f+\alpha_i/2)\mathbf{g}_{p_M}^H(f-\alpha_i/2) \\ &+ N_0\delta(\alpha_i)\mathbf{I}_{MN}. \end{aligned} \quad (112)$$

Consequently

$$\begin{aligned}\text{E}[|n_{M,w}^2(k)|] &= \frac{\pi_b}{T}\sum_{1\leq p\leq P}\sum_{\alpha_i}\int \mathbf{w}_M^H(f+\alpha_i/2) \\ &\mathbf{g}_{p,M}(f+\alpha_i/2)\mathbf{g}_{p_M}^H(f-\alpha_i/2)\mathbf{w}_M(f-\alpha_i/2)df \\ &+ N_0\int\|\mathbf{w}_M(f)\|^2df. \end{aligned} \quad (113)$$

This gives after direct algebraic manipulations, the following expressions of the MSE

$$\begin{aligned}\text{MSE} &= \pi_b T\int_\Delta |1-\frac{1}{T}\sum_k \mathbf{w}_M^H(f-\frac{k}{T})\mathbf{g}_M(f-\frac{k}{T})|^2df \\ &+ \int_\Delta \frac{\pi_b}{T}\sum_{1\leq p\leq P}\sum_\ell\sum_k \mathbf{w}_M^H(f-\frac{k}{T}) \\ &\qquad \mathbf{g}_{p,M}(f-\frac{k}{T})\mathbf{g}_{p,M}^H(f-\frac{\ell}{T})\mathbf{w}_M(f-\frac{\ell}{T})df \\ &+ N_0\int_\Delta\sum_k\|\mathbf{w}_M(f-\frac{k}{T})\|^2df. \end{aligned} \quad (114)$$

This MSE is a quadratic functional of $\mathbf{w}_M(f-\frac{k}{T})$, $k\in\mathbb{Z}$. Similarly to the JMSE, using a variational method, the MSE (114) is minimized by

$$\mathbf{w}_{M_o}(f) = c_{M,1}^d(f)\mathbf{g}_M(f)+\sum_{1\leq p\leq P}c_{M,1+p}^d(f)\mathbf{g}_{p,M}(f) \quad (115)$$

where $(c_{M,1}^d(f),c_{M,2}^d(f),..,c_{M,1+P}^d(f))^T$ is the first column of $\mathbf{C}_{M_o}^d(f)=[\frac{N_0}{\pi_b}\mathbf{I}_{P+1}+\frac{1}{T}\sum_\ell \mathbf{G}_M^H(f-\frac{\ell}{T})\mathbf{G}_M(f-\frac{\ell}{T})]^{-1}$. ■

2) Proof of (26)*:* Using the approach consisting to jointly estimate the SOI and MUI symbols $\mathbf{b}_n \overset{\text{def}}{=} [b_n,b_{1,n},..b_{P,n}]^T$, the filter $\mathbf{w}_3^*(-t)$ minimizing the MSE criterion corresponds to the first column of the $3N\times(P+1)$ matrix $\mathbf{W}_3^*(-t)$ filter whose output is $\mathbf{y}_3(t)=\mathbf{W}_3^H(-t)\otimes\mathbf{x}_3(t)$. This filter minimizes the joint MSE criterion: $\text{JMSE}=\text{E}(\|\mathbf{b}_n-\mathbf{y}_3(nT)\|^2)$. Following the steps of the proof of (25) given in Appendix B, where contrary to the two-input signal $\mathbf{x}_2(t)$, the CT background noise output $\mathbf{W}_3^*(-t)\otimes\boldsymbol{\epsilon}_3(t)$ is SO cyclostationary with cyclic frequencies $\alpha_i\in\{-\frac{1}{T},0,+\frac{1}{T}\}$, the JMSE criterion is given by:

$$\begin{aligned}\text{JMSE} &= \pi_b T\int_\Delta \text{Tr}\big[\big(\mathbf{I}_{P+1}-\frac{1}{T}\sum_\ell \mathbf{W}_3^H(f-\frac{\ell}{T}) \\ &\mathbf{G}_3(f-\frac{\ell}{T})\big)\big(\mathbf{I}_{P+1}-\frac{1}{T}\sum_\ell \mathbf{W}_3^H(f-\frac{\ell}{T})\mathbf{G}_3(f-\frac{\ell}{T})\big)^H\big]df \\ &+\int_\Delta \text{Tr}\big[\sum_{i=-1,0,+1}\sum_k \mathbf{W}_3^H(f-\frac{k}{T})\mathbf{R}_{\epsilon_3}^{\alpha_i}(f)\mathbf{W}_3(f-\frac{k+i}{T})\big]df \end{aligned} \quad (116)$$

This JMSE is a quadratic functional of $\mathbf{W}_3(f-\frac{k}{T})$, $k\in\mathbb{Z}$. Following a standard method of the calculus of variations (see e.g., [42]), this JMSE (116) is minimized by the unique

solution in $\mathbf{W}_3(f)$ of the following equation:

$$\pi_b \mathbf{G}_3(f)\left[\mathbf{I}_{P+1} - \frac{1}{T}\sum_{\ell}\mathbf{G}_3^H(f-\frac{\ell}{T})\mathbf{W}_3(f-\frac{\ell}{T})\right] = \sum_{i=-1,0,+1}\mathbf{R}_{\epsilon_3}^{\alpha_i}(f)\mathbf{W}_3(f-\alpha_i). \quad (117)$$

Noting that $\sum_{i=-1,0,+1}\mathbf{R}_{\epsilon_3}^{\alpha_i}(f)\mathbf{W}_3(f-\alpha_i) = \mathbf{W}_3(f) + + \begin{pmatrix} \mathbf{0}_{N,P+1} \\ \mathbf{W}_{3,3}(f+\frac{1}{T}) \\ \mathbf{W}_{3,2}(f-\frac{1}{T}) \end{pmatrix}$ with $\mathbf{W}_3(f) \stackrel{\text{def}}{=} \begin{pmatrix} \mathbf{W}_{3,1}(f) \\ \mathbf{W}_{3,2}(f) \\ \mathbf{W}_{3,3}(f) \end{pmatrix}$, it s straightforward to show that

$$\mathbf{W}_3(f) = \begin{bmatrix} \mathbf{G}_2(f)\mathbf{C}_{2_o}^d(f) \\ \mathbf{0}_{N,P+1} \end{bmatrix} \text{ is solution of (117).} \quad \blacksquare$$

3) Proof of (50) *and* (51)*:* The first component of $\mathbf{y}_M(k)$ (108) is given by

$$\begin{aligned} y_M(k) &= b_k(\mathbf{f}^T\mathbf{U}_{M_o}(0)\mathbf{f}) + \mathbf{f}^T\mathbf{U}_{M_o}(0)(\mathbf{b}_k - b_k\mathbf{f}) \\ &+ \sum_{\ell\neq k}\mathbf{f}^T\mathbf{U}_{M_o}(k-\ell)\mathbf{b}_\ell + \mathbf{f}^T\boldsymbol{\epsilon}_{w,M}(k) \\ &\stackrel{\text{def}}{=} b_k(\mathbf{f}^T\mathbf{U}_{M_o}(0)\mathbf{f}) + e_M(k), \end{aligned} \quad (118)$$

where b_k and $e_M(k)$ are uncorrelated and $\mathbf{U}_{M_o}(0)$ is given from the definition of $\mathbf{C}_M^d(f)$ in $\mathbf{w}_{M_o}(f)$ (25) by

$$\begin{aligned} \mathbf{U}_{M_o}(0) &= \int_\Delta \mathbf{C}_M^d(f)\sum_\ell \mathbf{G}_M^H(f-\frac{\ell}{T})\mathbf{G}_M(f-\frac{\ell}{T})df \\ &= \mathbf{I}_{P+1} - \frac{N_0T}{\pi_b}\int_\Delta \mathbf{C}_M^d(f)df. \end{aligned} \quad (119)$$

Noting that $\mathbf{U}_{M_o}(0)$ is Hermitian, the expressions of $\mathrm{E}(|e_M(k)|^2)$ and $\mathrm{E}(e_M^2(k))$ are given by:

$$\begin{aligned} \mathrm{E}(|e_M(k)|^2) &= \pi_b\mathbf{f}^T[\sum_\ell \mathbf{U}_{M_o}(\ell)\mathbf{U}_{M_o}^H(\ell)]\mathbf{f} \\ &-\pi_b(\mathbf{f}^T\mathbf{U}_{M_o}(0)\mathbf{f})^2 + \mathbf{f}^T\mathrm{E}[\boldsymbol{\epsilon}_{w,M}(k)\boldsymbol{\epsilon}_{w,M}^H(k))]\mathbf{f} \quad (120) \\ \mathrm{E}(e_M^2(k)) &= \pi_b\mathbf{f}^T[\sum_\ell \mathbf{U}_{M_o}(\ell)\mathbf{U}_{M_o}^T(\ell)]\mathbf{f} \\ -\pi_b(\mathbf{f}^T\mathbf{U}_{M_o}(0)\mathbf{f})^2 &+ \delta(M-2)\mathbf{f}^T\mathrm{E}[\boldsymbol{\epsilon}_{w,M}(k)\boldsymbol{\epsilon}_{w,M}^T(k))]\mathbf{f}, \quad (121) \end{aligned}$$

where

$$\begin{aligned} \sum_\ell \mathbf{U}_{M_o}(\ell)\mathbf{U}_{M_o}^H(\ell) &= T\int_\Delta(\sum_k \mathbf{U}_{M_o}(k)e^{-j2\pi fkT}) \\ &(\sum_\ell \mathbf{U}_{M_o}^H(\ell)e^{j2\pi f\ell T})df \quad (122) \\ \sum_\ell \mathbf{U}_{M_o}(\ell)\mathbf{U}_{M_o}^T(\ell)) &= T\int_\Delta(\sum_k \mathbf{U}_{M_o}(k)e^{-j2\pi fkT}) \\ &(\sum_\ell \mathbf{U}_{M_o}^T(\ell)e^{j2\pi f\ell T})df \quad (123) \end{aligned}$$

with

$$\begin{aligned} &\sum_k \mathbf{U}_{M_o}(k)e^{-j2\pi fkT} \\ &= \frac{1}{T}\sum_\ell \mathbf{W}_{M_o}^H(f-\frac{\ell}{T})\mathbf{G}_M(f-\frac{\ell}{T}) \\ &= \frac{1}{T}\mathbf{C}_M^d(f)[\sum_\ell \mathbf{G}_M^H(f-\frac{\ell}{T})\mathbf{G}_M(f-\frac{\ell}{T})] \\ &= (\mathbf{I}_{P+1} - \frac{N_0}{\pi_b})\mathbf{C}_M^d(f). \end{aligned} \quad (124)$$

Using

$$\begin{aligned} &\mathrm{E}[\boldsymbol{\epsilon}_{w,M}(k)\boldsymbol{\epsilon}_{w,M}^H(k))] \\ &= N_0\int \mathbf{W}_{M_o}^H(f)\mathbf{W}_{M_o}(f)df \\ &= N_0\int_\Delta \mathbf{C}_M^d(f)[\sum_\ell \mathbf{G}_M^H(f-\frac{\ell}{T})\mathbf{G}_M(f-\frac{\ell}{T})]\mathbf{C}_M^d(f)df \\ &= N_0T\int_\Delta[\mathbf{C}_M^d(f) - \frac{N_0}{\pi_b}\mathbf{C}_M^d(f)\mathbf{C}_M^d(f)]df \end{aligned} \quad (125)$$

and

$$\begin{aligned} &\mathrm{E}[\boldsymbol{\epsilon}_{w,M}(k)\boldsymbol{\epsilon}_{w,M}^T(k))] \\ &= \delta(M-2)N_0\int \mathbf{W}_{M_o}^H(f)\mathbf{J}_{2N}\mathbf{W}_{M_o}^*(-f)df \\ &= N_0T\int_\Delta[\mathbf{C}_M^d(f) - \frac{N_0}{\pi_b}\mathbf{C}_M^d(f)\mathbf{C}_M^d(f)]df \end{aligned} \quad (126)$$

where we have used in (126) for $M = 2$, the relations $\mathbf{J}_{2N}\mathbf{G}_M(-f) = \mathbf{G}_M^*(f)$ and $\mathbf{C}_M^{d^*}(-f) = \mathbf{C}_M^d(f)$.

Gathering (125), (122) with (124) in (120), and (126), (123) with (124) in (121), the generic expression of the SINR (41) takes the value (50). For $M = 2$, using $\mathbf{f}^T\mathbf{C}_M^d(f)\mathbf{C}_M^d(f)\mathbf{f} = \mathbf{f}^T\mathbf{C}_M^d(f)\mathbf{C}_M^{d^*}(-f)\mathbf{f} = \|\mathbf{C}_M^d(f)\mathbf{f}\|^2$, (50) reduces to (51). $\blacksquare$

C. Proofs related to the s M-input MMSE receivers

1) Proof of (30)*:* The output, at time kT of the filter $\mathbf{w}_M^*(f)$ is given by the SO stationary signal:

$$y_M(k) = u_M(0)b_k + \sum_{\ell\neq k}u_M(k-\ell)b_\ell + n_{w,M}(k), \quad (127)$$

where $u_M(\ell) \stackrel{\text{def}}{=} \int \mathbf{w}_M^H(f)\mathbf{g}_M(f)e^{j2\pi f\ell T}df$ and $n_{w,M}(k) \stackrel{\text{def}}{=} \int \mathbf{w}_M^H(f)\mathbf{n}_M(f)e^{j2\pi fkT}df$ where $\mathbf{n}_M(t)$ is falsely assumed SO stationary with power spectral density $\mathbf{R}_{n,M}^0(f)$. Following the same steps as that of the derivation of (109), we get the MSE

$$\begin{aligned} \mathrm{MSE} &\stackrel{\text{def}}{=} \mathrm{E}|y_k - b_k|^2 \\ &= \pi_bT\int_\Delta \left|1 - \frac{1}{T}\sum_\ell \mathbf{w}_M^H(f-\frac{\ell}{T})\mathbf{g}_M(f-\frac{\ell}{T})\right|^2 df \\ &+ \int_\Delta \sum_k \mathbf{w}_M^H(f-\frac{k}{T})\mathbf{R}_{n_M}^{(0)}(f-\frac{k}{T})\mathbf{w}_M(f-\frac{k}{T})df, \end{aligned} \quad (128)$$

whose function in the global integral (128) is classically minimized by $\mathbf{w}_{M_s}(f)$ given by (30). ■

D. Proofs related to SINR of s three-input MMSE receivers

1) Proofs of (77), (78)*:* To derive closed-form expressions of the SINR, it is easier to calculate the powers $P_{\rm SOI}$, $P_{\rm ISI}$, $P_{\rm MUI}$ and $P_{\rm BN}$ of the different terms of (96) than to use the global formulas (46) and (**??**)

$$\mathrm{SINR}_{3_s} = \frac{P_{\rm SOI}}{P_{\rm ISI}+P_{\rm MUI}+P_{\rm BN}}, \tag{129}$$

where the different powers are given by

$$P_{\rm SOI} = \pi_b \left[\int_\Delta \sum_k \mathbf{w}_{3_s}^H(f-\frac{k}{T})\mathbf{g}_3(f-\frac{k}{T})df\right]^2 \tag{130}$$

$$\begin{aligned} P_{\rm ISI} &= \frac{\pi_b}{2T}\left(\int_\Delta |\sum_k \mathbf{w}_{3_s}^H(f-\frac{k}{T})\mathbf{g}_3(f-\frac{k}{T})|^2 df\right. \\ &+ \left.\mathrm{Re}\left[\int_\Delta (\sum_k \mathbf{w}_{3_s}^H(f-\frac{k}{T})\mathbf{g}_3(f-\frac{k}{T})) \right.\right. \\ &\left.\left. (\sum_\ell \mathbf{w}_{3_s}^H(-f-\frac{\ell}{T})\mathbf{g}_3(-f-\frac{\ell}{T}))df\right]\right) \\ &- \pi_b\left[\int_\Delta \sum_k \mathbf{w}_{3_s}^H(f-\frac{k}{T})\mathbf{g}_3(f-\frac{k}{T})df\right]^2 \end{aligned} \tag{131}$$

$$\begin{aligned} P_{\rm MUI} &= \frac{\pi_b}{2T}\left(\int_\Delta |\sum_k \mathbf{w}_{3_s}^H(f-\frac{k}{T})\mathbf{g}_{1,3}(f-\frac{k}{T})|^2 df\right. \\ &+ \left.\mathrm{Re}\left[\int_\Delta (\sum_k \mathbf{w}_{3_s}^H(f-\frac{k}{T})\mathbf{g}_{1,3}(f-\frac{k}{T})) \right.\right. \\ &\left.\left. (\sum_\ell \mathbf{w}_{3_s}^H(-f-\frac{\ell}{T})\mathbf{g}_{1,3}(-f-\frac{\ell}{T}))df\right]\right) \end{aligned} \tag{132}$$

$$\begin{aligned} P_{\rm BN} &= \frac{1}{2}\left(\sum_{\alpha\in A}\int \mathbf{w}_{3_s}^H(f+\frac{\alpha}{2})\mathbf{R}_{\epsilon_3}^{\alpha}(f)\mathbf{w}_{3_s}(f-\frac{\alpha}{2})\right. \\ &+ \left.\sum_{\beta\in B}\int \mathbf{w}_{3_s}^H(f+\frac{\beta}{2})\mathbf{C}_{\epsilon_3}^{\beta}(f)\mathbf{w}_{3_s}^*(-f+\frac{\beta}{2})\right) \end{aligned} \tag{133}$$

where $A \stackrel{\rm def}{=} \{1/T, 0, +1/T\}$ and $B \stackrel{\rm def}{=} \{-1/T, 0\}$. Including the filter $\mathbf{w}_{3_s}(f)$ (30) in (130)-(133) allows us to derive after cumbersome algebraic manipulations:

$$P_{R,\rm SOI} = \frac{c^2}{\pi_b}\epsilon_s^2\left(3-\frac{|\alpha_{s,1}|^2\epsilon_1}{1+\epsilon_1}-\frac{4|\alpha_{s,1}|^2\epsilon_1\cos^2\phi_{s,1}}{1+2\epsilon_1}\right)^2 \tag{134}$$

$$P_{R,\rm ISI} = 0 \tag{135}$$

$$\begin{aligned} P_{R,\rm MUI} &= \frac{c^2}{\pi_b}|\alpha_{s,1}|^2\epsilon_s\epsilon_1\cos^2\phi_{s,1}\left(\frac{4}{(1+2\epsilon_1)^2}\right. \\ &+ \left.\frac{1}{(1+\epsilon_1)^2}+\frac{4}{(1+\epsilon_1)(1+2\epsilon_1)}\right) \end{aligned} \tag{136}$$

$$\begin{aligned} P_{R,\rm BN} &= \frac{c^2}{\pi_b}\frac{\epsilon_s}{2}\left(9+|\alpha_{s,1}|^2\epsilon_1\left(\frac{\epsilon_1}{(1+\epsilon_1)^2}\right.\right. \\ &- \left.\left.\frac{6}{1+\epsilon_1}-\frac{8(2\epsilon_1^2+6\epsilon_1+3)}{(1+2\epsilon_1)^2)(1+\epsilon_1)}\cos^2\phi_{s,1}\right)\right) \end{aligned} \tag{137}$$

with

$$c \stackrel{\rm def}{=} \pi_b\left(1+\epsilon_s\left(3-\frac{|\alpha_{s,1}|^2\epsilon_1}{1+\epsilon_1}-\frac{4|\alpha_{s,1}|^2\epsilon_1\cos^2\phi_{s,1}}{1+2\epsilon_1}\right)\right)^{-1} \tag{138}$$

for R signals and

$$\begin{aligned} P_{QR,\rm SOI} &= \pi_b\left(1-\frac{1}{2\pi_b}(c_1+c_2)\right)^2 \\ &= \frac{\epsilon^2}{4\pi_b}\left[c_1\left(3-\frac{|\alpha_{s,1}|^2\epsilon_1}{1+\epsilon_1}-\frac{4|\alpha_{s,1}|^2\epsilon_1\cos^2\zeta_{s,1}}{1+2\epsilon_1}\right)\right. \\ &+ \left.c_2\left(3-\frac{|\alpha_{s,1}|^2\epsilon_1}{1+\epsilon_1}-\frac{4|\alpha_{s,1}|^2\epsilon_1\cos^2\psi_{s,1}}{1+2\epsilon_1}\right)\right]^2 \end{aligned} \tag{139}$$

$$\begin{aligned} P_{QR,\rm ISI} &= \frac{\epsilon^2}{2\pi_b}\left[c_1\left(3-\frac{|\alpha_{s,1}|^2\epsilon_1}{1+\epsilon_1}-\frac{4|\alpha_{s,1}|^2\epsilon_1\cos^2\zeta_{s,1}}{1+2\epsilon_1}\right)\right. \\ &- \left.c_2\left(3-\frac{|\alpha_{s,1}|^2\epsilon_1}{1+\epsilon_1}-\frac{4|\alpha_{s,1}|^2\epsilon_1\cos^2\psi_{s,1}}{1+2\epsilon_1}\right)\right]^2 \end{aligned} \tag{140}$$

$$\begin{aligned} P_{QR,\rm MUI} &= \frac{c_1^2}{2\pi_b}|\alpha_{s,1}|^2\epsilon_s\epsilon_1\cos^2\zeta_{s,1}\left(\frac{4}{(1+2\epsilon_1)^2}\right. \quad (141) \\ &+ \left.\frac{1}{(1+\epsilon_1)^2}+\frac{4}{(1+\epsilon_1)(1+2\epsilon_1)}\right) \\ &+ \frac{c_2^2}{2\pi_b}|\alpha_{s,1}|^2\epsilon_s\epsilon_1\cos^2\psi_{s,1}\left(\frac{4}{(1+2\epsilon_1)^2}\right. \quad (142) \\ &+ \left.\frac{1}{(1+\epsilon_1)^2}+\frac{4}{(1+\epsilon_1)(1+2\epsilon_1)}\right) \quad (143) \end{aligned}$$

$$\begin{aligned} P_{QR,\rm BN} &= \frac{c_1^2}{\pi_b}\frac{\epsilon_s}{4}\left(9+|\alpha_{s,1}|^2\epsilon_1\left(\frac{\epsilon_1}{(1+\epsilon_1)^2}\right.\right. \\ &- \left.\left.\frac{6}{1+\epsilon_1}-\frac{8(2\epsilon_1^2+6\epsilon_1+3)}{(1+2\epsilon_1)^2)(1+\epsilon_1)}\cos^2\zeta_{s,1}\right)\right) \\ &+ \frac{c_2^2}{\pi_b}\frac{\epsilon_s}{4}\left(9+|\alpha_{s,1}|^2\epsilon_1\left(\frac{\epsilon_1}{(1+\epsilon_1)^2}\right.\right. \\ &- \left.\left.\frac{6}{1+\epsilon_1}-\frac{8(2\epsilon_1^2+6\epsilon_1+3)}{(1+2\epsilon_1)^2)(1+\epsilon_1)}\cos^2\psi_{s,1}\right)\right) \end{aligned} \tag{144}$$

with

$$c_1 \stackrel{\text{def}}{=} \pi_b \left(1+\epsilon_s \left(3-\frac{|\alpha_{s,1}|^2\epsilon_1}{1+\epsilon_1}-\frac{4|\alpha_{s,1}|^2\epsilon_1\cos^2\zeta_{s,1}}{1+2\epsilon_1}\right)\right)^{-1} \quad (145)$$

$$c_2 \stackrel{\text{def}}{=} \pi_b \left(1+\epsilon_s \left(3-\frac{|\alpha_{s,1}|^2\epsilon_1}{1+\epsilon_1}-\frac{4|\alpha_{s,1}|^2\epsilon_1\cos^2\psi_{s,1}}{1+2\epsilon_1}\right)\right)^{-1} \quad (146)$$

for QR signals. From the expressions (134)-(146), we see that for $\tau_1 = 0$, $\cos^2\psi_{s,1} = \cos^2\zeta_{s,1}$, which implies $c_1 = c_2 = c$ and thus the powers of the different components of $z_{3_s}(k)$ for R and QR signals are equal and the associated SINR are equal. ■

E. Proofs related to the SER derivation

1) Proofs of the expressions of $\sigma^2_{\epsilon_{M_g}}$: For the o and s receivers with $M = 1, 2$ inputs, $\sigma^2_{\epsilon_{M_g}} = \frac{MN_0}{2}\int \|\mathbf{w}_{M_g}(f)\|^2 df$ and for the sc receiver $\sigma^2_{\epsilon_{M_{sc}}} = \frac{MN_0}{2}\int |v(f)|^2\|\mathbf{w}_{M_{sc}}(f)\|^2 df$ for R signals and $\sigma^2_{\epsilon_{M_{sc}}} = \frac{MN_0}{2}\int |v(f+4/T)|^2\|\mathbf{w}_{M_{sc}}(f)\|^2 df$ for QR signals. For the three-input receiver $\sigma^2_{\epsilon_{3_s}}$ is given by (133) where $\mathbf{R}^{\alpha}_{\epsilon_3}(f)$ and $\mathbf{C}^{\beta}_{\epsilon_3}(f)$ come from (52) and (53), respectively. ■

REFERENCES

[1] B. Picinbono and P. Chevalier, "Widely linear estimation with complex data," *IEEE Trans. Signal Process.*, vol. 43, no. 8, pp. 2030-2033, Aug. 1995.

[2] B. Picinbono, "On circularity," *IEEE Trans. Signal Process.*, vol. 42, no. 12, pp. 3473-3482, Dec 1994.

[3] Z. Ding and G. Li, "Single-Channel blind equalization for GSM cellular systems", *IEEE J. Sel. Areas Commun.*, vol. 16, no. 8, pp. 1493-1505, Oct. 1998.

[4] P. Chevalier and F. Pipon, "New insights into optimal widely linear array receivers for the demodulation of BPSK, MSK and GMSK signals corrupted by non circular interferences - Application to SAIC," *IEEE Trans. Signal Process.*, vol. 54, no. 3, pp. 870-883, March 2006.

[5] G. Gelli, L. Paura, and A.M. Tulino, "Cyclostationarity-based filtering for narrow-band interference suppression in direct-sequence spread spectrum systems", *IEEE J. Selected Areas Commun.*, vol 6, no. 9, pp. 1747-1755, Dec. 1998.

[6] S. Buzzi, M. Lops, and A. M. Tulino, "A new family of MMSE multiuser receivers for interference suppression in DS/CDMA systems employing BPSK modulation," *IEEE Trans. Commun.*, vol. 49, pp. 154-167, Jan. 2001.

[7] M. Konrad and W.H. Gerstacker, "Interference robust transmission for the downlink of an OFDM-Based mobile communications system," *EURASIP J. Wireless Commun. Netw.*, vol. 2008.

[8] N. Song, R.C. De Lamare, M. Haardt, and M. Wolf, "Adaptive widely linear reduced-rank interference suppression based on the multistage Wiener filter estimation", *IEEE Trans.Signal Process.*, vol. 60, no. 8, pp. 4003-4016, Aug. 2012.

[9] D. Mattera, L. Paura, and F. Sterle, "Widely linear MMSE equalizer for MIMO linear time-dispersive channel," *Electronic Letters*, vol. 39, no. 20, pp. 1481-1482, Oct. 2003.

[10] S. Buzzi, M. Lops, and S. Sardellitti, "Widely linear reception strategies for layered space-time wireless communications," *IEEE Trans. Signal Process.*, vol. 54, no. 6, pp. 2252-2262, Jun. 2006.

[11] P. Chevalier and F. Dupuy, "Widely linear Alamouti receivers for the reception of real-valued signals corrupted by interferences - The Alamouti SAIC/MAIC concept", *IEEE Trans. Signal Process.*, vol. 59, no. 7, pp. 3339-3354, July 2011.

[12] A. Mirbagheri, K.N. Plataniotis and S. Pasupathy, "An enhanced Widely Linear CDMA receiver with OQPSK modulation", *IEEE Trans. Commun.*, vol. 54, no. 2, pp. 261-272, Feb. 2006.

[13] H. Trigui and D.T.M. Slock, "Performance bounds for cochannel interference cancellation within the current GSM standard," *Signal Proccess., Elsevier*, vol. 80, pp. 1335-1346, 2000.

[14] R. Meyer, W.H. Gerstacker, R. Schober, and J.B. Huber, "A single antenna interference cancellation algorithm for increased GSM capacity", *IEEE Trans. Wireless Commun.*, vol. 5, no. 7, pp. 1616-1621, July 2006.

[15] M. Austin, "SAIC and synchronised networks for increased GSM capacity," in 3G Americas SAIC Working Group, Sep. 2003.

[16] A. Mostapha, R. Kobylinski, I. Kostanic, and M. Austin, "Single antenna interference cancellation (SAIC) for GSM networks", *IEEE Proc. Vehicular Technology Conf.*, vol. 2, pp. 1089-1093, Oct. 2004.

[17] W.H. Gerstacker, R. Schober, R. Meyer, F. Obernosterer, M. Ruder, and H. Kalveram, "GSM/EDGE: A mobile communications system determined to stay," *Inter. Journal Elec. Commun.*, vol. 65, pp. 694-700, 2011.

[18] M. Ruder, R. Meyer, F. Obernosterer, H. Kalveram, R. Schober, and W.H. Gerstacker, "Receiver concepts and resource allocation for OSC downlink transmission," *IEEE Trans. Wireless Commun.*, vol. 13, no. 3, pp. 1568-1581, March 2014.

[19] D. Molteni and M. Nicoli, "Joint OSC receiver for evolved GSM/EDGE," *IEEE Trans. Wireless Commun.*, vol. 12, no. 6, pp. 2608-2619, June 2013.

[20] W. Deng, Z. Li, Y. Xia, K. Wang, and W. Pei, "A Widely linear MMSE Anti-Collision method for multi-antenna RFID readers," *IEEE Commun. Letters*, vol 23, no. 4, pp. 664-647, Aug. 2019.

[21] R. Gui, N.M. Balasubramanya, and L. Lampe, "Connectivity performance evaluation for grant-free narrowband IoT with widely linear receivers," *IEEE Internet of Things Journal*, vol 7, no. 10, pp. 10562-10572, Oct. 2020.

[22] G.M. Swetha, K. Hemavathy, S. Natarajan, and V. Sambasiva, "Overcome message collisions in satellite automatic ID systems, *Microwave and RF, Systems*, May. 2018.

[23] M. Bavand and S.D. Blostein, "User selection and multiuser widely linear precoding for one-dimensional signalling," *IEEE Trans. Vehicular Technology*, vol. 67, no. 12, pp. 11642-11653, Dec. 2018.

[24] D. Tong, Y. Ding, Y. Liu, and Y. Wang, "A MIMO-NOMA framework with complex-valued power coefficients," *IEEE Trans. Vehicular Technology*, vol. 68, no. 3, pp. 2244?-259, March 2019.

[25] J.C. De Luna Ducoing, N. Yi, Y. Ma, and R. Tafazolli, "Using real constellations in fully-and over loaded large MU-MIMO systems with simple detection", *IEEE Wireless Commun. Letters*, vol. 5, no. 1, pp. 92-95, Feb. 2016.

[26] Y. Zeng, R. Zhang, and T.J. Lim, "Wireless Communications with unmanned aerial vehicles: Opportunities and challenges", *IEEE Commun. Mag.*, vol. 54, no. 5, pp. 36-42, May 2016.

[27] D. Darsena, G. Gelli, I. Iudice, and F. Verde, "Equalization techniques of control and non-payload communication links for unmanned aerial vehicles," *IEEE Access*, vol. 6, pp. 4485-4496, 2018.

[28] B. Farhang-Boroujeny and R. Kempter, "Multicarrier communication techniques for spectrum sensing and communication in cognitive radios," *IEEE Commun. Mag.*, vol. 46, no. 4, pp. 80-85, Apr. 2008.

[29] D. Chen, Y. Tian, D. Qu, and T. Jiang, "OQAM-OFDM for wireless communications in future internet of things: a survey on key technologies and challenges," *IEEE Internet of Things Journal*, vol. 5, no. 5, pp. 3788-3809, Oct. 2018.

[30] M. Caus and A.I. Perez-Neira, "Comparison of linear and widely linear processing in MIMO-FBMC systems," in *Proc. Int. Symp. Wireless Commun. Syst.*, pp. 21-25, Ilmenau, (Germany), Aug. 2013.

[31] Y. Chen and M. Haardt, "Widely linear processing in MIMO FBMC/OQAM systems," in *Proc. Int. Symp. Wireless Commun. Syst.*, pp. 743-747, Ilmenau, (Germany), Aug. 2013.

[32] A. Ishaque and G. Ascheid, "Widely linear receivers for SMT systems with TX/RX frequency-selective I/Q imbalance", in *Proc. Int. Symp. Personal, Indoor Mobile Radio Commun.*, pp. 800-805, 2014.

[33] P. Chevalier, R. Chauvat, and J.-P. Delmas, "Enhanced widely linear filtering to make quasi-rectilinear signals almost equivalent to rectilinear ones for SAIC/MAIC," *IEEE Trans. Signal Proces.*, vol. 66, no. 6, pp. 1438-1453, March 2018.

[34] P. Chevalier, R. Chauvat, and J.-P. Delmas, "Widely linear FRESH receivers for cancellation of data-like rectilinear and quasi-rectilinear

Interference with frequency-offsets,", *Signal Processing*, vol. 188, pp. 1-13, 108171, Nov., 2021.
[35] W.A. Gardner, "Cyclic Wiener filtering: theory and method," *IEEE Trans. Comm.*, vol. 41, no. 1, pp. 151-163, Jan. 1993.
[36] W.H. Gerstacker, R. Schober, and A. Lampe, "Receivers with widely linear processing for frequency-selective channels", *IEEE Trans. Commun.*, vol. 51, no. 9, pp. 1512-1523, Sept. 2003.
[37] P.A. Laurent, "Exact and approximate construction of digital phase modulations by superposition of amplitude modulated pulses (AMP)", *IEEE Trans. Commun.*, vol. 34, no. 2, pp. 150-160, Feb. 1986.
[38] J.G. Proakis, *Digital Communications*, Mc Graw Hill Series in Electrical and Computer Engineering, 4th Ed., 2001.
[39] W.A. Gardner, W.A. Brown, and C-K. Chen, "Spectral correlation of modulated signals: Part II - Digital modulation", *IEEE Trans. commun.*, vol. 35, no. 6, pp. 595-601, June 1987.
[40] D. Vucic and M. Obradovic, "Spectral correlation evaluation of MSK and offset QPSK modulation", *Signal Processing*, vol 78, pp. 363-367, 1999.
[41] P. Billingsley, *Probability and measure*, second edition, John Wiley and Sons, New-York, 1986.
[42] P. Balaban and J. Sack, "Optimum diversity combining and equalization in digital transmission with applications to cellular mobile radio - Part I: theoretical considerations", *IEEE Trans. commun.*, vol. 40, no. 5, pp. 885-894, May 1992.